Open access • Journal Article • DOI:10.1021/JA064521J

Charge instability in quadrupolar chromophores: symmetry breaking and solvatochromism. — Source link

Francesca Terenziani, Anna Painelli, Claudine Katan, Marina Charlot ...+1 more authors

Institutions: University of Rennes

Published on: 14 Nov 2006 - Journal of the American Chemical Society (American Chemical Society)

Topics: Explicit symmetry breaking and Symmetry breaking

Charge Instability in Quadrupolar Chromophores: Symmetry Breaking and Solvatochromism

Francesca Terenziani, Anna Painelli, Claudine Katan, Marina Charlot, Mireille Blanchard-Desce

Charge Instability in Quadrupolar Chromophores: Symmetry Breaking and Solvatochromism

Francesca Terenziani,[*,†] *Anna Painelli,*[†] *Claudine Katan,*[‡] *Marina Charlot,*[‡] *Mireille Blanchard-Desce*[‡]

Dipartimento di Chimica GIAF, Università di Parma & INSTM-UdR Parma, Parco Area delle Scienze 17/a, 43100 Parma, Italy; Synthèse et ElectroSynthèse Organiques, (CNRS, UMR 6510), Université de Rennes 1, Institut de Chimie, Campus Scientifique de Beaulieu, Bât 10A, 35042 Rennes Cedex, France.

AUTHOR EMAIL ADDRESS: francesca.terenziani@unipr.it

RECEIVED DATE (to be automatically inserted after your manuscript is accepted if required according to the journal that you are submitting your paper to)

TITLE RUNNING HEAD: Symmetry Breaking in Quadrupolar Chromophores

[†] Parma University.

[‡] Rennes 1 University.

J. AM. CHEM. SOC. 2006, 128, 15742-15755; DOI: 10.1021/ja064521j

ABSTRACT. We present a joint theoretical and experimental work aimed to understand the spectroscopic behavior of multipolar dyes of interest for NLO applications. In particular we focus on the occurrence of broken-symmetry states in quadrupolar organic dyes, and their spectroscopic consequences. In order to gain a unified description, we have developed a model based on a few-state description of the charge-transfer processes characterizing the low-energy physics of these systems. The model takes into account the coupling between electrons and slow degrees of freedom, namely molecular vibrations and polar solvation coordinates. We predict the occurrence of symmetry breaking in either the ground or the first excited state. In this respect, quadrupolar chromophores are classified in three different classes, with distinctively different spectroscopic behavior. Cases of true and false symmetry breaking are discriminated and discussed by making resort to non-adiabatic calculations. The theoretical model is applied to three representative quadrupolar chromophores: their qualitatively different solvatochromic properties are connected to the presence or the absence of broken-symmetry states, and related to TPA cross-sections. The proposed approach provides useful guidelines for the synthesis of dyes for TPA application and represents a general and unifying reference frame to understand energy transfer processes in multipolar molecular systems, offering important clues to understand basic properties of materials of interest for nonlinear optics and energy harvesting applications.

J. AM. CHEM. SOC. 2006, 128, 15742-15755; DOI: 10.1021/ja064521j

Introduction

Charge resonance is a characteristic feature of organic molecules where electron donor (D) and acceptor (A) groups are linked by π-conjugated bridges. Charge-transfer between D and A groups characterizes the low-energy physics of these molecules and is responsible for the appearance of low-energy excitations with large transition and/or mesomeric dipole moments.[1-3] Dipolar (D-π-A),[1-5] quadrupolar (D-π-A-π-D or A-π-D-π-A)[6-13] or, more generally, multipolar molecules[14-18] are therefore extensively investigated for applications in nonlinear optics (NLO). At the same time, since the low-energy excitations in these dyes imply large charge displacements, their linear and nonlinear optical spectra are strongly affected by the surrounding medium: dipolar and multipolar dyes with strong NLO responses are often good polarity probes.[2,17,19,20] The charge resonance implies a rearrangement of the electronic distribution in the molecule with important consequences on bond-orders and hence on the molecular geometry: vibrational and electronic degrees of freedom are strongly coupled, leading to important spectroscopic effects,[20-23] as well as to large vibrational contributions to NLO responses.[3,24-26] Charge resonance is also the fundamental process in charge-transfer complexes and salts,[27,28] i.e. systems where the charge-transfer interaction occurs between electron-donor and acceptor molecules, and in mixed-valence metallic complexes and chains, where electrons hop between metallic ions kept together by ligand groups.[29] Charge and structural instabilities and symmetry breaking phenomena have been quite extensively investigated in these systems as a consequence of electron-vibration coupling.[30-32] Here we propose the occurrence of similar phenomena in multipolar organic dyes.

A large body of experimental data is available for many families of quadrupolar[5,7,9-11,13,18,33-36] and octupolar chromophores[15,17,18,34,37-45] as well as for branched and dendritic systems.[16,40,43,44,46,47] Due to their highly symmetric structure, all these systems have no permanent dipole moment and of course vertical (unrelaxed) states are non-dipolar as well. However for many of these chromophores, experimental data suggest the existence of polar excited states. For example, strong fluorescence solvatochromism has been observed for quadrupolar and/or octupolar systems,[10,13,17,18,36,42,48,49] revealing the existence of highly

J. AM. CHEM. SOC. 2006, 128, 15742-15755; DOI: 10.1021/ja064521j

dipolar excited states. Time-resolved fluorescence anisotropy measurements suggest that the initially delocalized excitation may localize in the ps timescale over one branch of the chromophore, leading to the formation of a polar state.[38,44] Recent electroabsorption measurements[40,41] also point to the formation of dipolar excited states in 3-fold symmetric systems. The interpretation of this behavior is still controversial: quadrupolar (or multipolar) solvation has been proposed as responsible for the fluorescence solvatochromism;[13] localization or delocalization of excitations is a hotly debated topic for dendrons and branched compounds in general;[18,34,38,39,43-45,47] the interpretation of electroabsorption measurements is delicate and invokes structural disorder to explain the dipolar nature of the vertical excited state.[40,41]

In this paper we propose a general model for multipolar chromophores in solution, and apply it specifically to quadrupolar systems. The model, based on an essential-state description for the electronic system, accounts for electron-vibration coupling and for solvation effects. A detailed and internally consistent description of the ground state and of the (spectroscopically relevant) low-lying excited states is obtained in terms of the corresponding potential energy surfaces (PES). Multistable behavior shows up with multiple-minima PES. We investigate in detail the occurrence of charge instabilities and relaxation in either the ground or excited states. Full non-adiabatic diagonalization is adopted as a powerful and flexible computational tool for the simulation of linear and non-linear optical spectra. The approach is general and will be described in full detail in a forthcoming paper. Here we present the main features of the model for quadrupolar DAD or ADA chromophores, and validate it through an extensive comparison with experimental data. To such an aim a couple of chromophores have been synthesized and fully characterized as to provide stringent tests for the proposed model.

In the next Section we shortly introduce the model and show that, depending on the charge distribution on the molecule, bistable solutions can be expected in either the ground or the excited one-photon allowed states. Symmetry breaking and hence the dipolar nature of these states is then frozen due to the coupling to slow (vibrational and solvation) degrees of freedom. Spectroscopic consequences

J. AM. CHEM. SOC. 2006, 128, 15742-15755; DOI: 10.1021/ja064521j

of symmetry breaking are discussed, with special emphasis on absorption and/or fluorescence solvatochromism. The model is then validated against experiments. We present experimental data collected in solution for a newly synthesized fluorene-based chromophore that shows large two-photon absorption (TPA), solvent-independent one-photon absorption (OPA) spectra and a strongly solvatochromic fluorescence. This complex spectroscopic behavior is naturally explained by the proposed model. Similar behavior was indeed observed for other quadrupolar dyes, and the model is further validated by the comparison with published data on a different dye based on a tetrafluoro-benzene ring as the central A group. Finally, the case of a squaraine-based quadrupolar dye is discussed. We collect linear and non-linear spectra of this dye that barely shows no solvatochromism. This markedly different behavior is naturally described within the proposed model. The proposed model offers a microscopic picture for symmetry breaking in multipolar chromophores and rationalizes in a unifying reference scheme their variegated spectroscopic behavior. A classification of quadrupolar dyes emerges from this picture, offering a useful design tool for the synthesis of chromophores with desired properties.

Bistability and Symmetry Breaking: Model and Concepts

Charge resonance in D-π-A-π-D chromophores is described in chemical language as the resonance among three structures: $D^{+}A^{-}D \leftrightarrow DAD \leftrightarrow DA^{-}D^{+}$ (here and hereafter we will explicitly refer to D-π-A-π-D structures, but the same discussion applies to A-π-D-π-A chromophores, provided the role of D and A is interchanged). These states dominate the low-energy physics of the chromophores and suggest the use of a three-state picture to describe their electronic structure: indeed a three-state model has already been successfully adopted to describe quadrupolar donor-acceptor based compounds for NLO applications and to optimize their two-photon absorption cross-section.[50,51] However, the solvatochromism of quadrupolar dyes was not addressed in these papers. Here, for the first time, we extend the three-state electronic model to account at the same time for electron-vibration coupling and

J. AM. CHEM. SOC. 2006, 128, 15742-15755; DOI: 10.1021/ja064521j

for solvation effects. In the spirit of the Mulliken model,[27] that has been successfully applied to describe polar, D-π-A, chromophores (also known as push-pull chromophores),[20,21,25,52] the charge resonance model for quadrupolar chromophores is written on the basis of a set of three orthogonal states: $|N\rangle$, the neutral state, corresponding to the DAD structure, and two degenerate states, $|Z_1\rangle$ and $|Z_2\rangle$, corresponding to the two zwitterionic structures D^+A^-D and DA^-D^+, respectively. We define 2η as the energy difference between the two degenerate zwitterionic states and the neutral state, so that for positive η the neutral form is lower in energy than the zwitterionic forms, whereas the opposite occurs for negative η. The mixing between the states is described by an off-diagonal matrix element in the Hamiltonian, $\langle N|H|Z_1\rangle = \langle N|H|Z_2\rangle = -\sqrt{2}t$, that measures the probability of electron transfer from D to A and backwards. The direct mixing between Z_1 and Z_2 is set to zero, since it implies the direct hopping between non-nearest neighbor sites. The dipole moments associated with the two zwitterionic states point in opposite directions but have the same magnitude, μ_0, that is by far the largest matrix element of the dipole moment operator in the chosen basis: all other matrix elements of the dipole moment operator will be accordingly disregarded.

By exploiting inversion symmetry, we combine the zwitterionic states in symmetric and antisymmetric wavefunctions: $|Z_+\rangle = \frac{1}{\sqrt{2}}\left(|Z_1\rangle + |Z_2\rangle\right)$ and $|Z_-\rangle = \frac{1}{\sqrt{2}}\left(|Z_1\rangle - |Z_2\rangle\right)$, respectively. The N state is even, so that it only mixes to $|Z_+\rangle$. On the symmetrized basis (N, $|Z_+\rangle$ and $|Z_-\rangle$) the following three operators are conveniently defined:

$$\hat{\rho} = \begin{pmatrix} 0 & 0 & 0 \\ 0 & 1 & 0 \\ 0 & 0 & 1 \end{pmatrix}, \quad \hat{\delta} = \begin{pmatrix} 0 & 0 & 0 \\ 0 & 0 & 1 \\ 0 & 1 & 0 \end{pmatrix}, \quad \hat{\sigma} = \begin{pmatrix} 0 & 1 & 0 \\ 1 & 0 & 0 \\ 0 & 0 & 0 \end{pmatrix}, \qquad (1)$$

Here $\hat{\sigma}$ mixes the two *gerade* states; the two operators $\hat{\rho}$ and $\hat{\delta}$ define the charge distribution in the molecule: $\hat{\rho} = \hat{\rho}_1 + \hat{\rho}_2$ measures the average charge on the central A site, sum of the charges on the two external D sites; $\hat{\delta} = \hat{\rho}_1 - \hat{\rho}_2$ instead measures the unbalance of the charge on the two external (D) sites.

J. AM. CHEM. SOC. 2006, 128, 15742-15755; DOI: 10.1021/ja064521j

In terms of these operators, the representative matrices of the Hamiltonian and dipole moment operators are:

$$H_{el} = 2\eta\hat{\rho} - 2t\hat{\sigma}; \qquad \hat{\mu} = \mu_0\hat{\delta}. \tag{2}$$

The eigenstates of the Hamiltonian are easily obtained as:

$$\begin{aligned} |g\rangle &= \sqrt{1-\rho}\,|N\rangle + \sqrt{\rho}\,|Z_+\rangle \\ |c\rangle &= |Z_-\rangle \\ |e\rangle &= \sqrt{\rho}\,|N\rangle - \sqrt{1-\rho}\,|Z_+\rangle \end{aligned} \tag{3}$$

where ρ, the ground-state expectation value of the $\hat{\rho}$ operator, measures the weight of Z_+ in the ground state. The charge distribution in the ground state then corresponds to $D^{+0.5\rho}A^{-\rho}D^{+0.5\rho}$, so that ρ measures the quadrupolar character of the ground state. This important observable is fixed by the model parameters, as follows:

$$\rho = 0.5\left(1 - \eta/\sqrt{\eta^2 + 4t^2}\right) \tag{4}$$

The operator $\hat{\delta}$, proportional to the dipole moment operator, breaks the inversion symmetry and has vanishing expectation values in all states.

Transition energies and dipole moments can be expressed in terms of ρ:

$$\begin{aligned} \hbar\omega_{gc} &= \mathcal{E}_c - \mathcal{E}_g = 2t\sqrt{\frac{1-\rho}{\rho}}; & \mu_{gc} &= \langle g|\hat{\mu}|c\rangle = \mu_0\sqrt{\rho} \\ \hbar\omega_{ge} &= \mathcal{E}_e - \mathcal{E}_g = 2t\sqrt{\frac{1}{\rho(1-\rho)}}; & \mu_{ge} &= \langle g|\hat{\mu}|e\rangle = 0 \\ \hbar\omega_{ce} &= \mathcal{E}_e - \mathcal{E}_c = 2t\sqrt{\frac{\rho}{1-\rho}}; & \mu_{ce} &= \langle c|\hat{\mu}|e\rangle = -\mu_0\sqrt{1-\rho} \end{aligned} \tag{5}$$

The odd c state in eq (3) is one-photon (OP) allowed by symmetry, while the even e state is two-photon (TP) allowed from the ground state and OP allowed from the c state. For large positive η the ground state is largely dominated by the N state, $\rho \to 0$ and the one- and two-photon excitations become degenerate. In the opposite limit of large and negative η, the ground state is zwitterionic ($\rho \to 1$), the

J. AM. CHEM. SOC. 2006, 128, 15742-15755; DOI: 10.1021/ja064521j

OP excitation energy goes to zero (the ground state becomes degenerate) whereas the TP allowed state has a higher energy (-2η). The other notable case is $\eta = 0$, where $\rho = 0.5$, and the *c* state is located just midway between the *g* and *e* states.

The coupling between electronic and vibrational degrees of freedom is related to the different geometry associated with the neutral and zwitterionic states, much as it occurs for polar D-π-A chromophores.[25] The charge rearrangement from *N* to Z_1 or to Z_2 states occurs along the two (left and right) arms of the quadrupolar molecule, so that we introduce two mutually decoupled effective coordinates, q_1 and q_2, describing the nuclear motion in each arm. The two coordinates are equivalent by symmetry, and have the same harmonic frequency, ω. To describe the linear electron-vibration coupling we introduce a vibrational relaxation energy, ε_v, relevant to the two (equivalent) $N \rightarrow Z_1$ or $N \rightarrow Z_2$ processes. The relevant Hamiltonian reads:

$$H = H_{el} - \sqrt{2\varepsilon_v}\,\omega q_1 \hat{\rho}_1 - \sqrt{2\varepsilon_v}\,\omega q_2 \hat{\rho}_2 + \frac{1}{2}\left(\omega^2 q_1^2 + p_1^2\right) + \frac{1}{2}\left(\omega^2 q_2^2 + p_2^2\right) \qquad (6)$$

where, p_1 and p_2 are the momentum operators conjugate with q_1 and q_2, respectively. By exploiting inversion symmetry, we define the symmetric and antisymmetric coordinates:

$$q_+ = \frac{1}{\sqrt{2}}\left(q_1 + q_2\right); \qquad q_- = \frac{1}{\sqrt{2}}\left(q_1 - q_2\right) \qquad (7)$$

and conjugate momenta, p_+ and p_-. Hamiltonian in eq (6) then reads:

$$H = H_{el} - \sqrt{\varepsilon_v}\,\omega q_+ \hat{\rho} - \sqrt{\varepsilon_v}\,\omega q_- \hat{\delta} + \frac{1}{2}\left(\omega^2 q_+^2 + p_+^2\right) + \frac{1}{2}\left(\omega^2 q_-^2 + p_-^2\right) \qquad (8)$$

From this Hamiltonian one immediately recognizes the different role played by the symmetric and antisymmetric vibrations: q_+ is coupled to $\hat{\rho}$, so that oscillations along q_+ modulate the mixing between *N* and Z_+ and hence the amount of charge transferred in a symmetrical way from D to A. On the opposite, q_- is coupled to the antisymmetric $\hat{\delta}$ operator: oscillations along q_- induce a mixing of the symmetric *N* and Z_+ states with the antisymmetric Z_- state, driving an unbalance of the charge on the two external sites. In the adiabatic approximation one neglects the vibrational kinetic energy (terms

J. AM. CHEM. SOC. 2006, 128, 15742-15755; DOI: 10.1021/ja064521j

proportional to squared vibrational momenta, p_+^2, p_-^2 in eq (8)) to define an electronic Hamiltonian where vibrational coordinates enter as classical variables. Since q_- mixes states with different symmetry, Z_- is no more decoupled and one has to make resort to numerical techniques to diagonalize the 3 by 3 matrix. Diagonalization leads to three eigenstates that, much as the Hamiltonian, depend on q_+ and q_-. The corresponding energies, functions of the two vibrational coordinates, define the potential energy surfaces (PES) for the nuclear motion and contain all the information needed to describe optical spectra as well as symmetry-breaking phenomena.

Stable eigenstates with respect to symmetry breaking show a single minimum located at $q_- = 0$ and $q_+ = \sqrt{\varepsilon_v}\langle\rho\rangle/\omega$, where $\langle\rho\rangle$ is the expectation value of $\hat{\rho}$ in the relevant state. Unstable eigenstates instead show a double minimum structure: the symmetrical $q_- = \delta = 0$ solution corresponds to a saddle point in the PES, i.e. to an unstable state. Two equivalent minima at finite and opposite q_- values ($q_- = \pm\sqrt{\varepsilon_v}\langle\delta\rangle/\omega$) define two equivalent stable solutions, that correspond to broken-symmetry, and hence polar, states.

Figure 1 shows the relevant phase diagram where systems can be located as a function of ρ, the ground-state quadrupolar moment, and ε_v, the strength of electron-vibration coupling. The lines in the phase diagram mark values of the ρ and ε_v parameters for which the PES of the ground state (rightmost line) or the PES of the OP excited state (leftmost line) have zero curvature along the q_- coordinate, while the q_+ coordinate is fixed at its equilibrium value for the ground state. These boundaries distinguish three different regions, as schematically shown by the PES sketched in each region. Typical organic chromophores have ε_v values of the order of 0.5 or less ($\sqrt{2}t$ units).[20,23,51,53,54] In the central region (denoted as **II**), corresponding to systems with intermediate quadrupolar moment ($\rho \sim 0.3$-0.6), all three states have single-minimum PES: dyes belonging to region **II** have stable non-dipolar ground and excited states. In the leftmost region (**I**), corresponding to systems with low quadrupolar moment ($\rho < \sim 0.2$), the OP state, c, is bistable for sufficiently large ε_v values. In this region, the $q_- = 0$, $\delta = 0$

J. AM. CHEM. SOC. 2006, 128, 15742-15755; DOI: 10.1021/ja064521j

solution is unstable for the c state, so that symmetry can be broken towards one of two equivalent minima corresponding to states with equal and opposite δ, and hence equal and opposite dipole moments. Chromophores belonging to class **I** have non-dipolar ground state and second excited state (e, the TP state, is undistorted in the whole region of parameters) but the OP allowed state is polar when it localizes in one of the minima. In the third region of the phase diagram (**III**), corresponding to systems with a large quadrupolar moment ($\rho \rightarrow 1$) and large enough ε_v, both the OP and TP states are stable as non-polar, but the ground state is bistable.

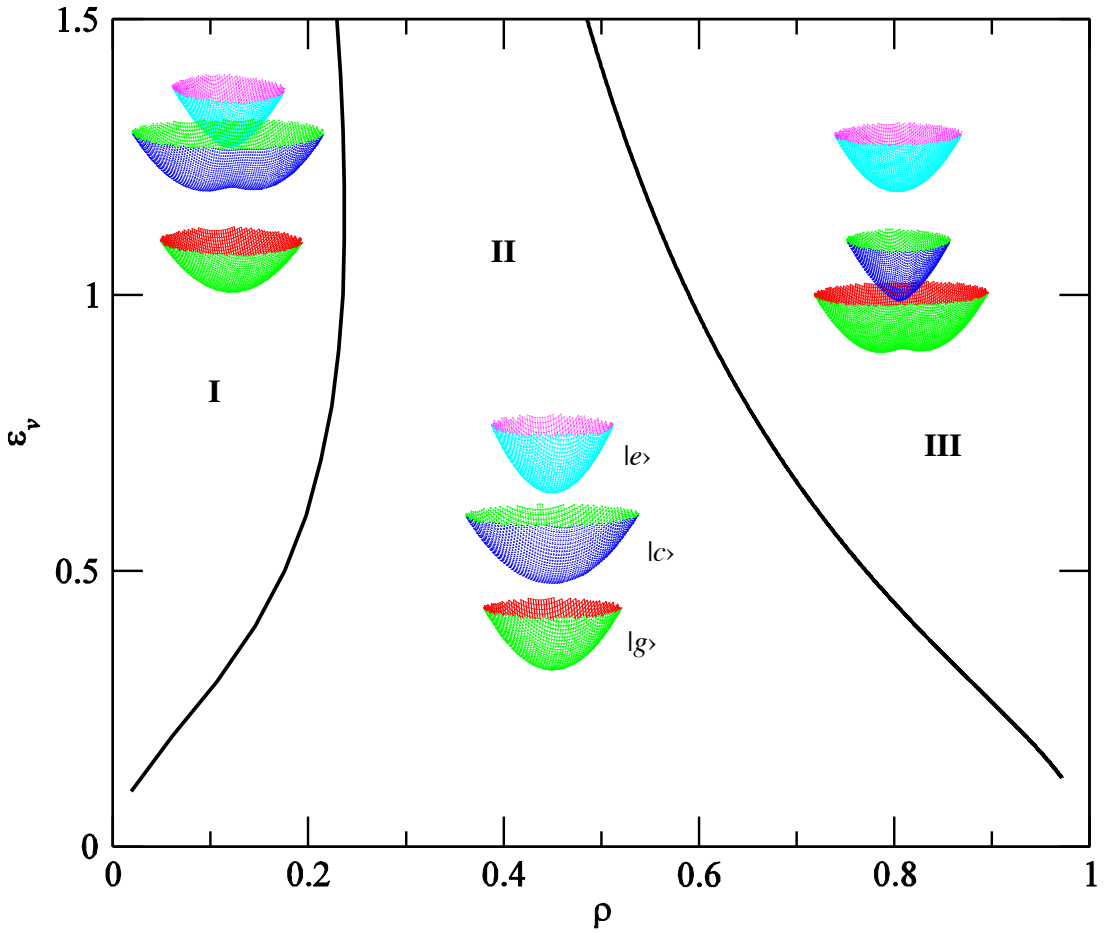

Figure 1. The phase diagram for quadrupolar chromophores, describing the stability of the different states (according to the PES sketched in each region) as a function of ρ (the quadrupolar character) and ε_v (the electron-vibration coupling, in units of $\sqrt{2}t$). The three PES in each region show, in order of increasing energy, the ground state (g), the OP state (c), and the TP state (e). Region **I**: stable ground state and bistable OP state; region **II**: all PES have a single minimum; region **III**: the ground-state PES

J. AM. CHEM. SOC. 2006, 128, 15742-15755; DOI: 10.1021/ja064521j

has a double minimum. The TP state always has a single minimum.

The phase-diagram in Figure 1 can be rationalized as follows. For $\rho \rightarrow 0$ the ground state corresponds to the almost pure N state, and the two excited states correspond to Z_- and Z_+. In this limit Z_- and Z_+ are almost degenerate and whatever tiny ε_v induces a symmetry breaking in the excited state. In the $\rho \rightarrow 1$ limit, Z_- and Z_+ are lower in energy than N, and the ground state almost coincides with Z_+. The ground state is therefore almost degenerate with the optically allowed state (Z_-) leading to a charge-instability in the ground state itself.

Symmetry breaking in molecular systems (i.e. in finite systems, as opposed to systems, like solids with infinite size) is a complex phenomenon that has been extensively discussed in the literature.[31,32,55] One of the basic problems is to discriminate between *true symmetry breaking*, where the system is localized in one of the two minima of the PES, from *false symmetry breaking* where, in spite of having a double-minimum PES, the symmetry is recovered due to the fast switching (tunneling) of the system between the two minima. This is a very interesting fundamental problem; here we concentrate on the calculation of optical spectra, and to avoid any ambiguity about false symmetry-breaking effects in the adiabatic solution, all spectral properties will be calculated from the direct non-adiabatic solution of the coupled electron-phonon problem.[26,31,56] Computational details are given in the Experimental Section.

The Hamiltonian in eq (8) describes the low-energy behavior of quadrupolar chromophores in non-polar solvents. In polar solvents additional effects are expected related to the coupling of electronic degrees of freedom with the slow orientational motion of polar solvent molecules.[2,57] In the spirit of continuum solvation model, and adopting exactly the same approach originally developed for dipolar (D-π-A) systems,[20,23,58] we neglect the minor contributions from quadrupolar and higher order solvation terms, and account for dipolar solvation interaction in the framework of the reaction-field approach. Treating the solvent as an elastic medium, the relevant Hamiltonian reads:[58]

$$H_{solv} = -\mu_0 F_R \hat{\delta} + \frac{\mu_0^2}{4\varepsilon_{or}} F_R^2 , \qquad (9)$$

J. AM. CHEM. SOC. 2006, 128, 15742-15755; DOI: 10.1021/ja064521j

where F_R measures the reaction field, whose equilibrium value is proportional to the solute's dipole moment: $F_R^{(eq)} = \left(2\varepsilon_{or}/\mu_0^2\right)\langle\hat{\mu}\rangle$. Here $\langle\hat{\mu}\rangle$ is the expectation value of the dipole moment operator, $\hat{\mu} = \mu_0\hat{\delta}$. The parameter ε_{or} measures the solvent relaxation energy, i.e. the energy gained by solvent relaxation after the vertical $N \rightarrow Z_{1/2}$ process;[2,57] ε_{or} obviously increases with the solvent polarity. At first sight eq (9) might suggest that polar solvation is irrelevant for non-dipolar chromophores such as the quadrupolar systems discussed in this work. But when symmetry breaking occurs either in the ground or in the OP state, one ends up with dipolar states, and dipolar solvation becomes relevant. More importantly, F_R couples to the same dipolar operator, $\hat{\delta}$, as the q_- coordinate so that dipolar solvation *cooperates* with vibrational coupling to support symmetry breaking and dipolar distortion. This reasoning based on the physics of operators is in line with standard chemical intuition, suggesting that dipolar states are stabilized in polar environments.

To better understand the role of polar solvation in driving symmetry breaking, Figure 2 shows the PES for the *g* and *c* states for a chromophore with $\rho = 0.2$ and $\varepsilon_v = 0.2$ (class **II**). The upper panel refers to a non-polar solvent (ε_{or} =0), so that only the two coordinates q_+ and q_- are relevant. The lower panel refers to a polar solvent ($\varepsilon_{or} > 0$), where an additional coordinate, F_R, must be accounted for. For graphical reasons, also in this case the PES are drawn in the q_+q_- plane, while keeping F_R fixed at its local equilibrium value for the *c* state ($F_R = \left(2\varepsilon_{or}/\mu_0\right) < c \mid \hat{\delta} \mid c >$): the PES in the lower panel of Figure 2 are then relevant to steady-state fluorescence as occurring from the *relaxed* excited state. Incidentally, the PES relevant to absorption processes (vertical processes starting from the equilibrium ground state) are not affected by the solvent polarity and therefore coincide with the $\varepsilon_{or} = 0$ PES in the upper panel. As expected for a class **II** chromophore, the PES shown in the top panel of Figure 2 ($\varepsilon_{or} = 0$) describe stable non-polar *g* and *c* states. Specifically, the PES for the *c* state has a single minimum, located at $q_- = 0$ (as fixed by inversion symmetry) and finite $q_+ = \sqrt{\varepsilon_v}\langle c|\hat{\rho}|c\rangle/\omega$. However,

J. AM. CHEM. SOC. 2006, 128, 15742-15755; DOI: 10.1021/ja064521j

for large enough ε_{or} and for relaxed solvent configuration (i.e. fixing F_R at the equilibrium value for the excited state) the minimum of the excited-state PES moves in the q_+q_- plane, as expected for a state that breaks inversion symmetry (bottom panel of Figure 2). This state with finite q_- is characterized by a finite δ and hence the *relaxed c* state has a net dipole moment. Of course an equivalent minimum exists with opposite dipole moment and opposite F_R. So, as far as symmetry breaking is concerned, the *total relaxation energy* (vibrational + solvation contributions) is the key quantity: only when a threshold value for the total relaxation energy is reached, symmetry breaking occurs. This implies that for systems with a small ε_v, symmetry can be broken only for large ε_{or} and thus a marked fluorescence solvatochromism will be observed only in highly polar solvents.

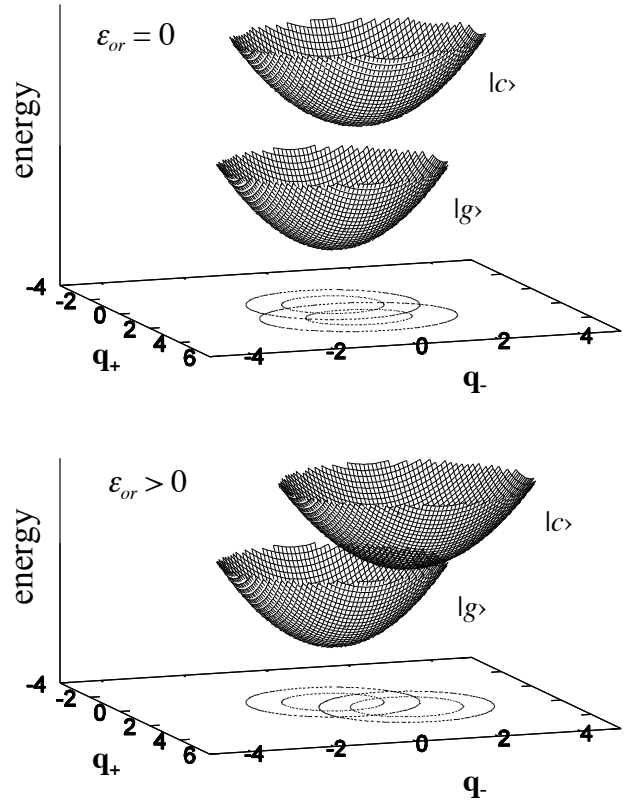

Figure 2. PES for the ground state and the OP-allowed excited state for a chromophore with $\rho = 0.2$, $\sqrt{2}t = 1$ eV and $\varepsilon_v = 0.2$ eV. Top panel: $\varepsilon_{or} = 0$ (apolar solvent); Bottom panel: $\varepsilon_{or} = 1$ eV (strongly dipolar solvent) and reaction field (F_R) fixed at its local equilibrium value for the *c* state.

J. AM. CHEM. SOC. 2006, 128, 15742-15755; DOI: 10.1021/ja064521j

For example, the system considered in Figure 2 breaks symmetry in the excited state only for $\varepsilon_{or} > 0.5$. The value of ε_{or} for a given solvent strongly depends on the dimension and shape of the solute molecule, being of the order of 0.5-1.0 eV for highly dipolar solvents (such as DMSO) and for a solute cavity relevant to typical push-pull chromophores (radius of the order of 5 Å).[20,23,54,58,59] For elongated molecules, such as typical quadrupolar (D-π-A-π-D or A-π-D-π-A) chromophores, the shape of the cavity is hardly approximated by a sphere, so that precise estimates are difficult. In any case, our model does not rely on any specific microscopic model for ε_{or}, but extracts its value from experimental data. We underline that not all systems belonging to class **II** undergo symmetry breaking as a result of polar solvation: for intermediate values of ρ (approximately $0.25 < \rho < 0.6$) symmetry breaking is not expected, at least for realistic ε_{or} values.

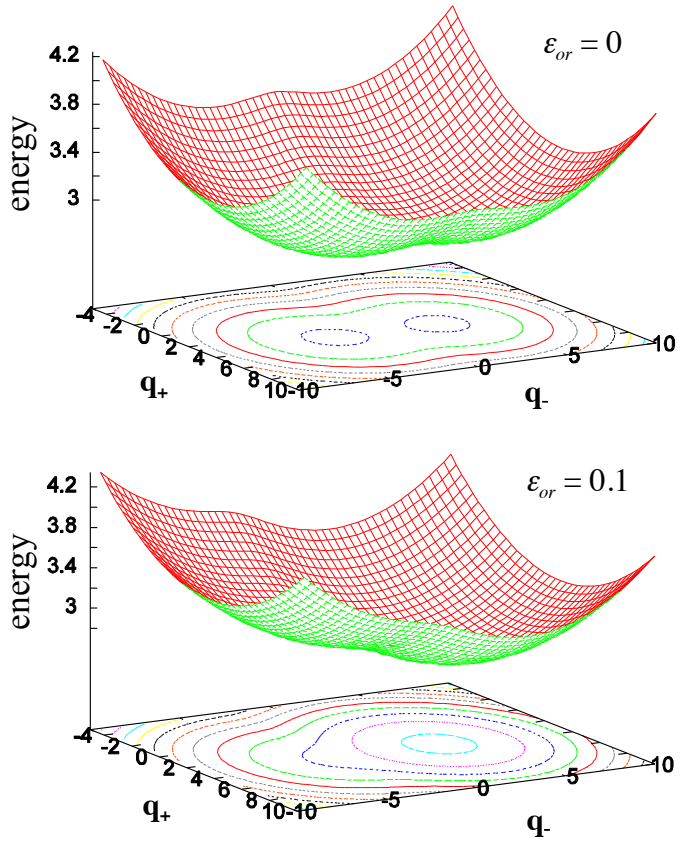

Figure 3. PES for the OP-allowed excited state for a class **I** chromophore with $\rho = 0.07$, $\sqrt{2}t = 0.6$ eV and $\varepsilon_v = 0.3$ eV. Top panel: $\varepsilon_{or} = 0$ (apolar solvent); Bottom panel: $\varepsilon_{or} = 0.1$ eV (low-medium polarity

J. AM. CHEM. SOC. 2006, 128, 15742-15755; DOI: 10.1021/ja064521j

solvent) and reaction field (F_R) fixed at its local equilibrium value for the *c* state.

A different case is shown in Figure 3 where we plot the PES relevant to state *c* for a chromophore with $\rho \approx 0.1$ and a large enough electron-vibration coupling ($\varepsilon_v = 0.5$ units of $\sqrt{2t}$) as to lead to a double-minimum PES (class **I**) already in non-polar solvents (top panel, $\varepsilon_{or} = 0$). In this case, already in slightly polar solvents (small ε_{or}, bottom panel), a sizeable stabilization of the polar broken-symmetry state is expected: important fluorescence solvatochromism is thus predicted already in weakly polar solvents. Of course an equivalent "mirror image" minimum as the one described in the bottom panel of Figure 3 develops at opposite q_- and F_R values.

It is important to realize that the *vertical* excited state always maintains the symmetry of the ground state, so that for chromophores having a centrosymmetric ground state (class **I** and **II**) absorption frequencies are basically unaffected by polar solvation (only inhomogeneous broadening effects are expected in absorption bands, as discussed in the analysis of chromophore **1**). On the opposite, steady state fluorescence occurs from the relaxed *c*-state, that for class **I** chromophores is polar (at least in polar solvents): large positive fluorescence solvatochromism is thus expected. PES in Figure 3 also help to underline the different role played by vibrational and solvation degrees of freedom with respect to symmetry breaking. As discussed above, both polar solvation and vibrational coupling have similar effects (and indeed cooperate) in favoring the appearance of double-minima (bistable) PES. However solvation and vibrational motions have very different time-scales: vibrational coordinates (typically in the mid infrared region) describe a truly quantum mechanical motion, so that, depending on the height of the barrier between the two minima, a fast interconversion (tunneling) between the two broken-symmetry states may restore the original symmetry (the false symmetry breaking case).[55] Instead polar solvation can be described in terms of a very slow (actually overdamped) coordinate, that behaves as a classical coordinate[60] and therefore does not support tunneling. In other words, interconversion between the two equivalent broken-symmetry minima is extremely slow in polar solvents since it requires the

J. AM. CHEM. SOC. 2006, 128, 15742-15755; DOI: 10.1021/ja064521j

motion along a slow classical coordinate. Of course both minima (i.e. both solute-solvent conformations) are equally probable and hence are equally populated: relevant spectra are however exactly the same and simply sum up in spectra calculated as Boltzmann averages over solvation coordinates[20,23] (see also Calculation Details in the Experimental Section).

Symmetry Breaking in Action: Fluorescence Solvatochromism

As already anticipated, several examples are reported in the literature of quadrupolar chromophores exhibiting strongly solvatochromic fluorescence.[10,13,18,36,48] In these systems a benzenoid structure typically corresponds to the *N* resonating form. The quinoidal structures associated with either Z_1 or Z_2 have therefore a much higher energy ($2\eta >> 0$) and their contribution to the ground state is small: these chromophores have small quadrupolar moments (approximately $\rho < 0.2$) and belong to class **I**. In this Section we will discuss in detail linear absorption and fluorescence spectra as well as two-photon absorption spectra for two specific chromophores of this kind, to assess and clearly identify the spectroscopic effects of bistability and symmetry breaking.

Example 1. The first example is a newly synthesized chromophore (**1**), sketched in Figure 4, characterized by two external electron-donor amino groups and a central fluorene core acting as an electron-acceptor moiety.[12,61].

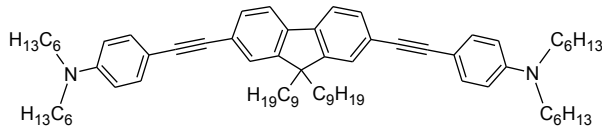

Figure 4. Molecular structure of compound **1**.

Table 1. Solvation effects on photophysical properties of **1**.

J. AM. CHEM. SOC. 2006, 128, 15742-15755; DOI: 10.1021/ja064521j

Solvent	λ_{abs} (nm)	λ_{em} (nm)	Stokes-shift (cm^{-1})	Dielectric constant [a]	τ [b] (ns)	Φ [c]	τ_0 [d] (ns)
Toluene	387	421	2100	2.4	0.74	0.80	0.93
$CHCl_3$	389	433	2600	4.8	0.80	0.86	0.93
Hexanol	385	450	3600	13.3	0.93	0.83	1.12
Acetone	387	482	5100	20.7	1.42	0.83	1.72
CH_3CN	388	503	5900	37.5	1.67	0.96	1.75

[a] Solvent dielectric constant at 20 °C. [b] Measured fluorescence lifetime. [c] Fluorescence quantum yield. [d] Radiative lifetime derived as $\tau_0 = \tau/\Phi$.

Photophysical properties of chromophore **1** dissolved in solvents of increasing polarity are summarized in Table 1; experimental absorption and fluorescence spectra are shown in Figure 5a; Figure 5b shows the two-photon absorption (TPA) spectrum collected in toluene. Molecule **1** shows a marked fluorescence solvatochromism, while the absorption spectrum is almost independent of the solvent polarity. The TPA spectrum presents a weak shoulder in correspondence with the transition towards the OP allowed state, and a second strong transition corresponding to the *e* state, whose maximum is located beyond the experimentally accessible spectral region.

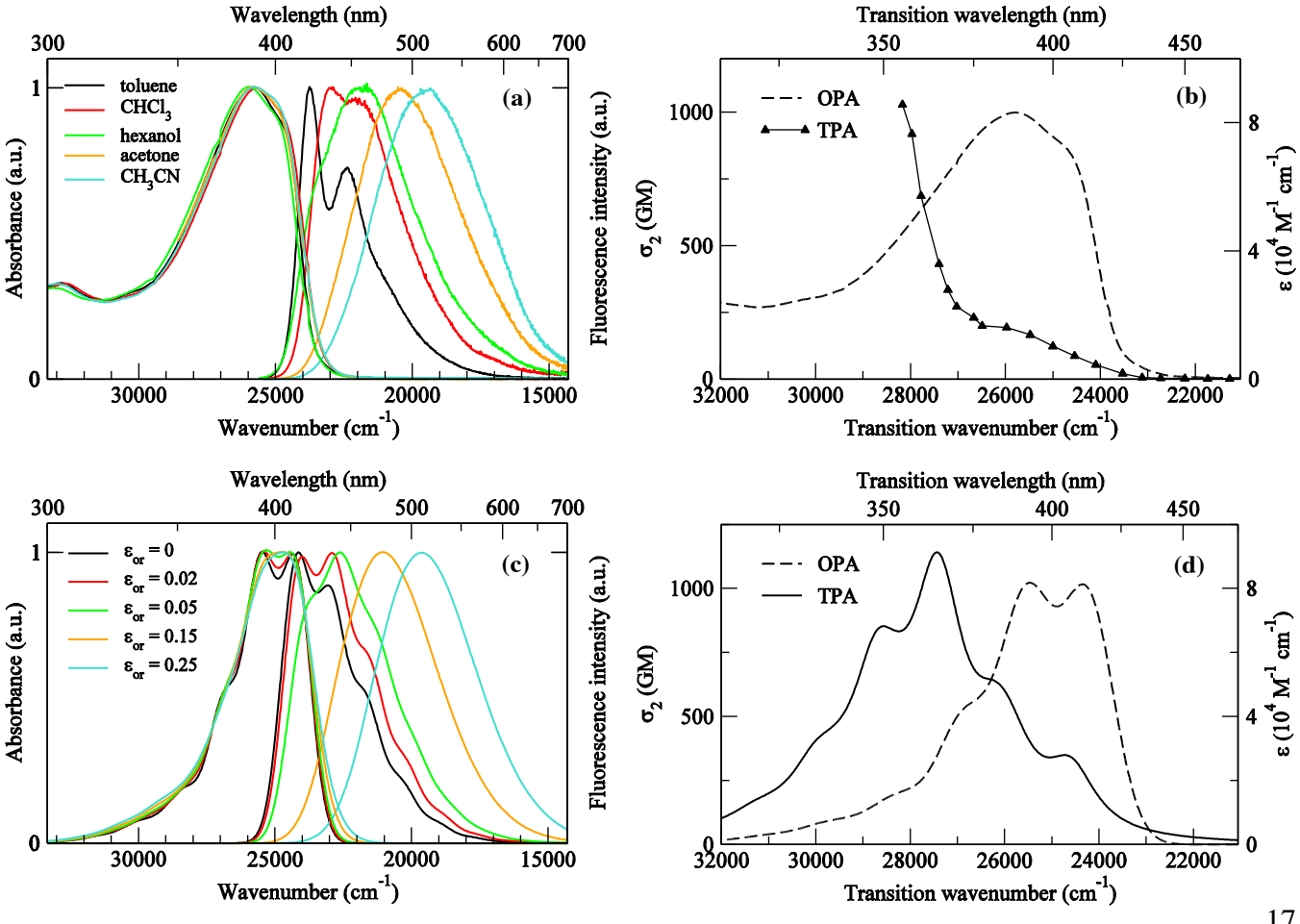

J. AM. CHEM. SOC. 2006, 128, 15742-15755; DOI: 10.1021/ja064521j

Figure 5. Spectra of compound **1**. Left panels: experimental (a) and calculated (c) absorption and fluorescence spectra in solvents of increasing polarity. Right panels: experimental (b) and calculated (d) one- and two-photon absorption spectra of **1** in toluene. 1 GM = 10^{-50} cm^4 s $photon^{-1}$. Calculated spectra have been obtained by fixing the following parameters: $\eta = 1.50$ eV, $\sqrt{2}t = 0.60$ eV, $\omega_v = 0.16$ eV, $\varepsilon_v = 0.30$ eV, HWHM = 0.08 eV, $\mu_0 = 40$ D. Values for ε_{or} in the legend (eV).

These data can be used to test the proposed model and shed light on the photophysical behavior of the chromophore. Molecular model parameters can be readily estimated from spectroscopic data in the non-polar solvent (toluene). The frequencies of the maximum of the linear absorption and TPA (ω_{gc} and ω_{ge}, respectively) fix ρ and $\sqrt{2}t$ (and hence η, see eqs (4)).

The TPA maximum is not experimentally accessible, but we locate it between 700 and 720 nm (transition wavelength between 350 and 360 nm) by comparison with data on related chromophores.[8,11,62,63] The molecular parameters describing vibrational coupling, ω_v, ε_v, are fixed as to reproduce the Frank-Condon progression in the absorption (or fluorescence) spectrum. Finally, the band-width (HWHM) associated to each transition is estimated from experimental spectra, and μ_0 is fixed to correctly reproduce the measured extinction coefficient. This procedure allows to calculate the spectra reported in Figure 5, panels c and d, relevant to toluene (black lines). Spectra in other solvents are obtained by introducing the solvation term in our Hamiltonian, and tuning the *single* parameter ε_{or} that accounts for solvent polarity, while *all the molecular parameters are kept fixed independently of the solvent*. Colored lines in Figure 5c show spectra calculated for the ε_{or} values in the legend. Calculated spectra reproduce main experimental features. Specifically, the frequency of the absorption band is barely affected by the solvent polarity. The main effect of polar solvation is recognized in the inhomogeneous broadening of the absorption band: in agreement with experimental data, the vibronic structure, resolved in low-polarity solvents, is progressively smeared out with increasing solvent

J. AM. CHEM. SOC. 2006, 128, 15742-15755; DOI: 10.1021/ja064521j

polarity. We underline that the calculated broadening is a genuine result of our solvation model: the HWHM for the vibronic lines is in fact exactly the same for all calculated spectra. The strong solvatochromism observed in steady-state fluorescence is well reproduced by our model. Moreover calculated spectra also reproduce the evolution of the emission band-shape with the solvent polarity: in particular, the evolution of the Frank-Condon profile is described by our results, with a progressive borrowing of intensity of the 0-*n* vibronic transitions at the expense of the 0-0 line. Again this is a genuine result: ε_v is kept constant in all solvents. Whereas the model well reproduces the observed trends, small discrepancies are observed. The Stokes-shift calculated in the less polar solvent (toluene) is underestimated: this could be cured by assigning toluene a small ε_{or} value, as suggested by empirical polarity scales.[2,64] Conformational or torsional degrees of freedom represents another source of Stokes-shift in non-polar solvents and may also cure for the minor discrepancy between calculated and experimental line-shapes in toluene.[20,65]

Based on the analysis of spectroscopic data, chromophore **1** can be classified as a low-quadrupolar molecule ($\rho \approx 0.07$), and the relevant $\varepsilon_v = 0.5$ (units of $\sqrt{2}t$) clearly locates it in the **I** region of the phase diagram, where the *c* state PES has a double minimum even in non-polar solvents. Indeed the PES in Figure 3 are obtained for parameters relevant to **1**. The appearance of a double minimum *c*-PES already in non-polar solvents naturally explains the lack of mirror-image symmetry between absorption and fluorescence spectra measured in toluene. In fact, in the case of a double-minimum excited-state PES, the Franck-Condon factors can be significantly different for the absorption and the fluorescence processes: the absorption process occurs from the lowest vibrational eigenstates of the single-minimum ground-state towards the unrelaxed (Franck-Condon) eigenstates of the double-minimum excited-state PES, while the fluorescence process stems from the lowest vibrational eigenstate of the double-minimum excited-state PES to the (Franck-Condon) eigenstates of the single-minimum ground-state. The strong dependence of fluorescence spectra on the solvent polarity, even for solvents with very low-polarity (cf. spectra in toluene and chloroform in Figure 5) is also linked to the double-minimum nature

J. AM. CHEM. SOC. 2006, 128, 15742-15755; DOI: 10.1021/ja064521j

of the excited state. In fact, upon vertical absorption, the system reaches a bistable state, so that even a very weak perturbation as due to the interaction with a slightly dipolar solvent breaks the molecular symmetry and creates a polar excited state, stabilized in polar solvents. The evolution of the fluorescence frequency with the solvent polarity can be approximated as: $\hbar\omega_{cg} = \hbar\omega_{cg}^{(0)} - \mu_{cc}\Delta f / r^3$, where r is the cavity radius and $\Delta f = (\varepsilon - 1)/(2\varepsilon + 1) - (n^2 - 1)/(2n^2 + 1)$ is the solvent polarity indicator (ε and n are the solvent dielectric constant and refractive index, respectively).[66] If μ_{cc} was independent of the solvent polarity, a straight line would be obtained for ω_{cg} vs Δf. Instead, data in Figure 6a sharply deviate from linearity, suggesting a large variation of the dipole moment of the relaxed excited state with the solvent polarity.

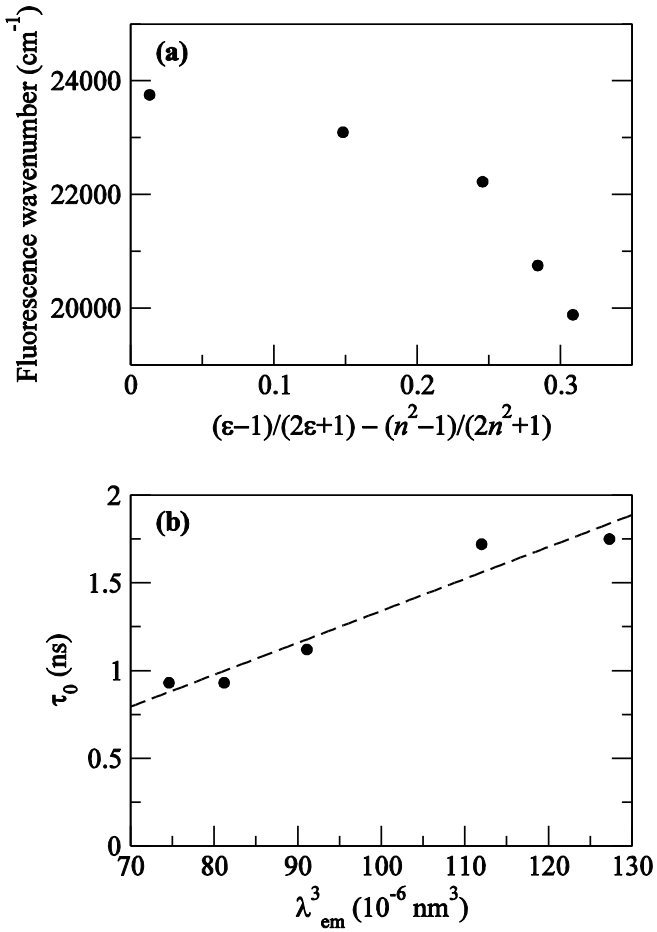

Figure 6. (a) Emission frequency of compound **1** vs. the solvent polarity indicator (ε is the dielectric constant and n the refractive index). (b) Radiative lifetime vs. λ_{em}^3 (points) and corresponding linear

J. AM. CHEM. SOC. 2006, 128, 15742-15755; DOI: 10.1021/ja064521j

regression (dashed line).

Based on the analysis of linear spectra of chromophore **1** we estimate the dipole moment for the relaxed excited state as $\mu_{cc} = 0$, 20, 33, 36, 37 D in toluene, $CHCl_3$, hexanol, acetone and CH_3CN, respectively. The relaxed excited state is non-polar in toluene (a case of false symmetry breaking) and acquires an increasing dipolar character (real symmetry breaking) with increasing solvent polarity, reaching an almost "saturated" value in hexanol, in qualitative agreement with data in Figure 6a. While a strong evolution of the dipole moment in the relaxed excited state is predicted and observed, only a ~ 20% variation of the squared transition dipole moment for the fluorescence process is calculated when going from apolar to highly polar solvents. If we consider the well-known relation $1/\tau_0 \propto \mu_{trans}^2 \omega_{trans}^3$,[67] we can easily verify that the solvent dependence of τ_0 can indeed be mainly ascribed to the solvent dependence of the fluorescence frequency (see Figure 6b) in agreement with calculated results.

TPA spectra also deserve some comments. The calculated TPA spectrum reported in Figure 5d compares favorably with experimental data (Figure 5b), even if a complete comparison is hindered by experimental limitations.[68] In the available spectral region, both the absolute value of the TPA cross section and the TPA band-shape are well reproduced. The TP *e*-state never undergoes symmetry breaking (see Figure 1). However, the coupling between electronic degrees of freedom and the antisymmetric vibrational coordinate (q_-) has interesting consequences on TPA spectra. In fact, the shoulder observed in the TPA spectrum in correspondence with the one-photon allowed state is quantitatively reproduced in our model, and can be assigned to the vibronic activation of the otherwise two-photon forbidden *c* state. Specifically, the two low-energy shoulders in the calculated TPA spectrum are assigned to a vibronic activation of the *c* state as a result of the coupling with antisymmetric q_- vibrations, while the successive more intense peaks correspond to genuine $g \rightarrow e$ transitions, with the 0-0 line being the strongest one. Our results, rule out alternative explanations based on the deviation of the molecular structure from linearity.

J. AM. CHEM. SOC. 2006, 128, 15742-15755; DOI: 10.1021/ja064521j

Example 2. As a second example we discuss results from Ref. [13] relevant to the centrosymmetric D-π-A-π-D molecule **2**, sketched in Figure 7.

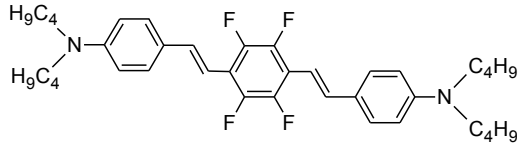

Figure 7. Molecular structure of compound **2**.

Much as for chromophore **1**, a strong solvatochromism is observed in fluorescence, whereas no dependence of the absorption band on the solvent polarity is reported. Interestingly, solvatochromic studies of the dipolar D-π-A analogue, show that the fluorescence solvatochromism of quadrupolar compound **2** is of the same order of magnitude than for the dipolar counterpart. In Ref. [13] this strong fluorescence solvatochromism was ascribed to solute quadrupole-solvent dipole interactions, following a formulation due to Suppan.[69] This formalism is however flawed: by symmetry reasons, a quadrupolar charge distribution cannot induce a *uniform* reaction field at the location of the solute. Of course, field gradients can occur at the solute location, but these cannot be described by introducing a single solvation coordinate (i.e. a uniform electric field). On physical grounds, these quadrupolar (or higher multipolar) contributions to solvation are expected to be much smaller than dipolar ones. We therefore suggest that the observed behavior is again due to symmetry breaking in the relaxed excited state as due to polar solvation. Following the same procedure already described for **1**, we estimate model parameters for chromophore **2**. The calculated absorption, fluorescence, and TPA spectra are reported in Figure 8, where black lines are relevant to the non-dipolar solvent, whereas colored lines refer to solvents of increasing polarity. These spectra are in good agreement with those reported in Ref. [13]: not only transition energies, and hence fluorescence solvatochromism, are well reproduced, but also band-shapes and absolute intensities of linear and two-photon absorption compare favorably with experimental data.

For **2** we estimate $\rho \approx 0.13$, i.e. a quadrupolar character which is almost twice that of **1**. Accordingly, we expect a less pronounced instability for the *c* state. Indeed for the adopted model parameters, the

J. AM. CHEM. SOC. 2006, 128, 15742-15755; DOI: 10.1021/ja064521j

PES relevant to the OP state presents a double minimum, but with a very low barrier (about half a vibrational quantum). This is the reason why absorption and fluorescence spectra in the non-polar solvent have very similar vibronic progressions (at variance with chromophore **1**, for which the barrier amounts to about 2 vibrational quanta). Again, the dipole moment calculated for the relaxed excited state of **2** vanishes in the non-polar solvent, to attain a sizeable value in THF (21 D) and CH_3CN (22 D). The calculated TPA spectrum presents two weak shoulders in correspondence to transition towards the one-photon allowed state (see Figure 8b): this phenomenon is again due to a weak vibronic activation of the *c* state. The experimental spectrum does not allow to conclude if this feature is actually present. In any case, these vibronic bands in the TPA spectrum are calculated much less intense than for **1**, a phenomenon that is again due to the stronger quadrupolar character of **2**.

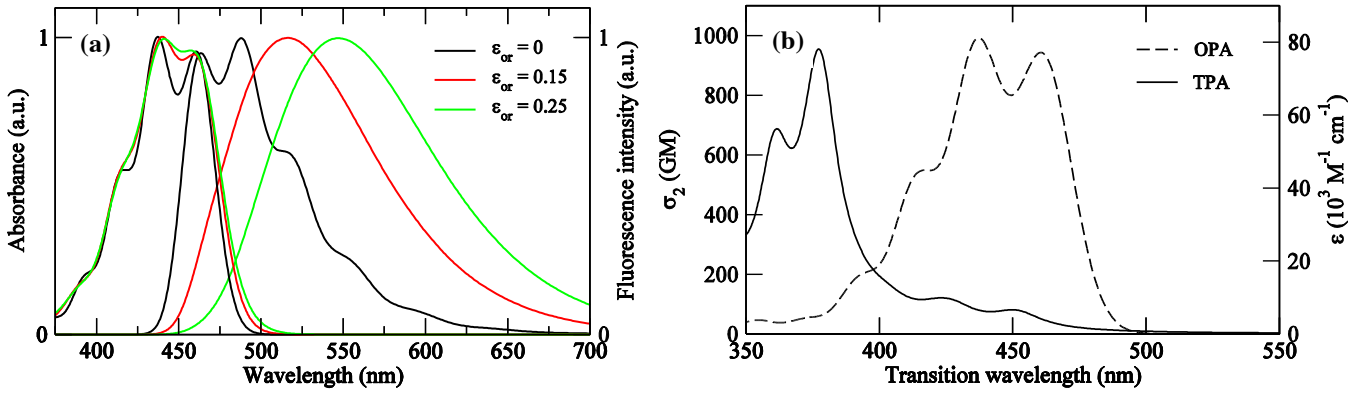

Figure 8. Calculated spectra for compound **2**. (a) Absorption and fluorescence in solvents of increasing polarity; (b) one- and two-photon absorption in apolar solvent. Calculated spectra have been obtained by fixing the following parameters: $\eta = 1.25$ eV, $\sqrt{2}t = 0.80$ eV, $\omega_v = 0.15$ eV, $\varepsilon_v = 0.42$ eV, HWHM = 0.07 eV, $\mu_0 = 28$ D. Values for ε_{or} in the legend (eV).

Highly-quadrupolar, symmetry-preserving systems

Squaraine-based quadrupolar dyes show minor solvatochromism both in absorption and fluorescence.[70] For these chromophores only one study of two-photon absorption is available in the literature, reporting data collected with nanosecond excitation pulses.[35] To obtain more reliable data, we

J. AM. CHEM. SOC. 2006, 128, 15742-15755; DOI: 10.1021/ja064521j

have synthesized a squaraine-dye (**3** in Figure 9). Absorption and fluorescence spectra of **3** have been collected in several solvents and its TPA spectra have been measured using femtosecond pumping, as to minimize spurious contributions due to long pulse duration.

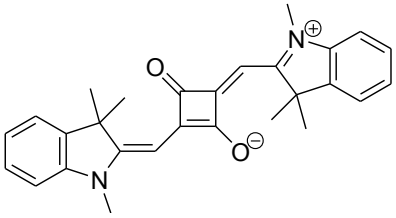

Figure 9. Molecular structure of compound **3**.

Photophysical properties of **3** are summarized in Table 2. Absorption and fluorescence spectra, as well as the TPA profiles of **3** in solvents of different polarity are shown in Figure 10, panel (a) and (b), respectively. Linear spectra confirm that chromophore **3** is only marginally solvatochromic, both in absorption and in emission (10 nm excursion in a wide range of solvent polarity). As for TPA spectra in $CHCl_3$ we confirm results in Ref. [35], with a maximum at 820 nm, even if the actual cross section is about 40% lower than reported in Ref. [35] (in which TPA measurements were conducted using nanosecond pumping). Measurements in other solvents however suggest that the peak at 820 nm does not correspond to the maximum of the TPA band but that the TPA signal increases further in the region below 800 nm that, quite unfortunately, is not accessible with our experimental setup. Indeed results reported in Ref. [13] for two squaraine-based dyes (there labeled 13a and 13e) having similar structures, indicate cross sections differing by an order of magnitude: this discrepancy can be understood at the light of our data, suggesting that the band at 820 nm is just a shoulder of a probably much more intense two-photon transition placed below 800 nm. While this is quite clear from our measurements in toluene and DMSO solutions, the increase of σ_2 with respect to the 820 nm maximum is not detected for the $CHCl_3$ solution when moving down to 800 nm (Figure 10b). The different behavior in $CHCl_3$ with respect to toluene and DMSO can be ascribed to a small blue-shift of the band (see linear absorption

J. AM. CHEM. SOC. 2006, 128, 15742-15755; DOI: 10.1021/ja064521j

spectra) or to possible photodegradation problems (as suggested by the fact that the dependence of the TPEF response on the incident intensity is quadratic only for low intensities in that particular solvent).

Table 2. Photophysical properties of **3** in solvents of different polarity.

Solvent	Dielectric constant	Refractive index	λ_{abs} (nm)	λ_{em} (nm)	Stokes-shift (cm^{-1})	ε (cm^{-1} M^{-1})	Φ
Toluene	2.38	1.497	639	648	215	330 000	0.66
$CHCl_3$	4.81	1.446	633	642	235	305 000	0.43
DMSO	46.7	1.478	641	652	265	280 000	0.20

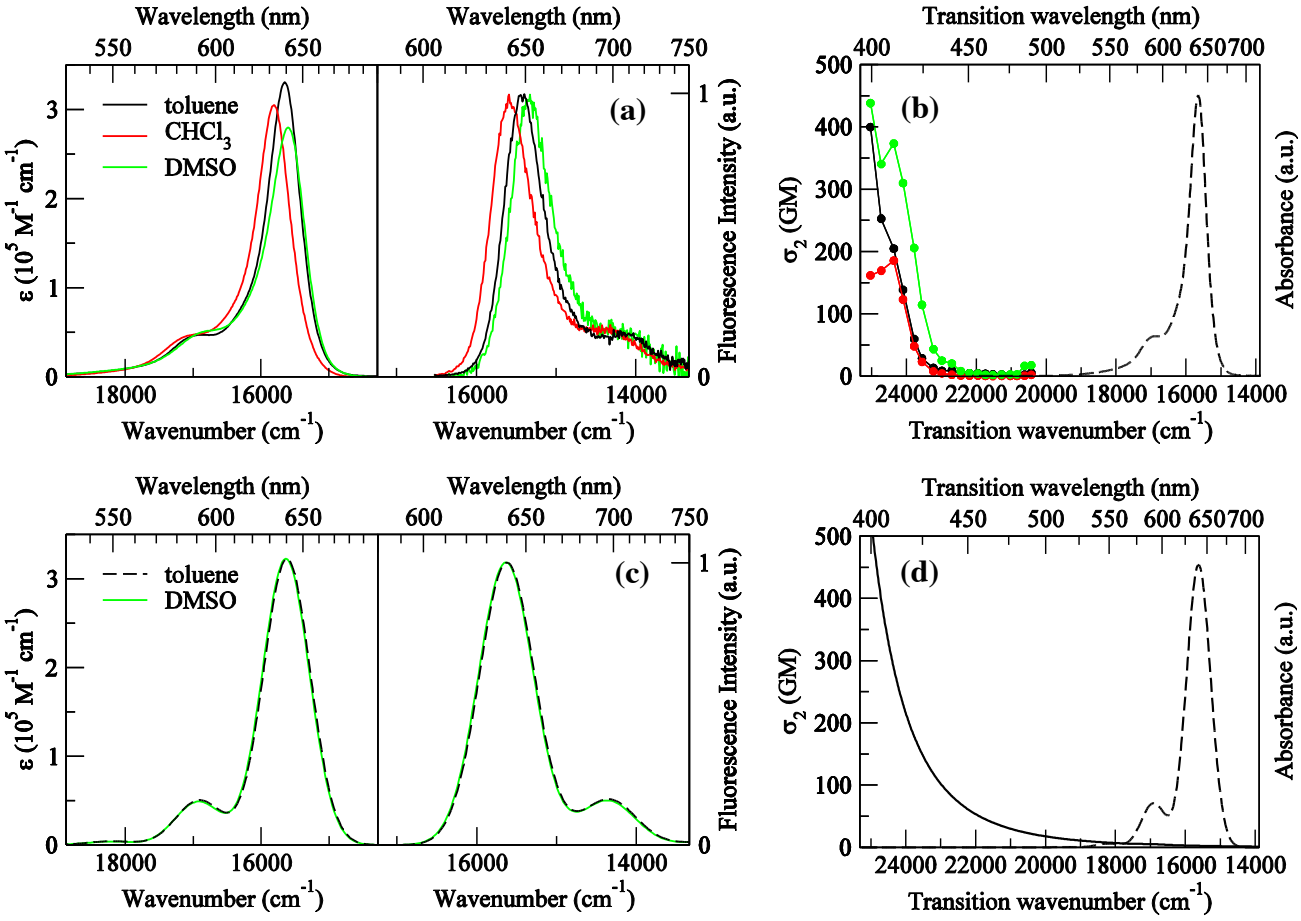

Figure 10. Spectra of compound **3**. Top panels: experimental absorption and fluorescence (a) and TPA spectra (b) in solvents of increasing polarity (the OPA spectrum in toluene is reported for comparison).

J. AM. CHEM. SOC. 2006, 128, 15742-15755; DOI: 10.1021/ja064521j

Bottom panels: calculated absorption and fluorescence in two solvents of different polarity (c) and TPA spectrum in apolar solvent (d) (the OPA spectrum is reported for comparison). Calculated spectra have been obtained by fixing the following parameters: $\eta = 0.28$ eV, $\sqrt{2}t = 1.20$ eV, $\omega_v = 0.16$ eV, $\varepsilon_v = 0.16$ eV, HWHM = 0.05 eV, $\mu_0 = 21$ D; $\varepsilon_{or} = 0, 0.25$ eV for toluene and DMSO, respectively.

In any case, fixing the TPA frequency between 800 and 700 nm, and making use of linear absorption data, we obtain a crude estimate of the model. Specifically, we estimate $\rho \approx 0.4$ and $\varepsilon_v \approx 0.13$ (units of $\sqrt{2}t$), so that squaraine **3** can be located in region **II** of the phase diagram in Figure 1, suggesting that for this chromophore all states of interest for spectroscopy maintain a non-dipolar character. In these conditions, solvation effects are not able to break the symmetry of the system. This explains why no noticeable solvatochromism is observed either in absorption or in fluorescence spectra. The observation of a residual weak solvatochromism can be attributed to the difference in the solvent refractive indexes (see Table 2). Moreover, at variance with chromophores of class **I**, inhomogeneous broadening is not effective in absorption nor in emission spectra. This confirms the large quadrupolar character of **3**, since for dyes with large ρ (approximately $\rho > 0.2$) the dependence of the transition frequency on ρ is smooth, leading to negligible inhomogeneous broadening effects.

The same analysis can be extended to chromophore 13e in Ref. [35], for which we estimate $\rho \approx 0.3$, with a TPA cross section of the order of 9.000 GM, in reasonable agreement with the reported one. This squaraine dye is then also placed in region **II** of the phase diagram in Figure 1, with no symmetry breaking phenomena in either the ground state or excited state.

Discussion and Conclusions

This paper represents a joint theoretical and experimental work aimed to understand the interesting and variegated spectroscopic behavior of quadrupolar dyes, an interesting family of molecules for NLO

J. AM. CHEM. SOC. 2006, 128, 15742-15755; DOI: 10.1021/ja064521j

applications. These chromophores represent typical examples of molecules where the coupling between electronic and vibrational degrees of freedom play a significant role in governing their optical responses (in the ground and/or excited states). The coupling between electronic and vibrational degrees of freedom indeed governs structural instabilities in a variety of extended systems with delocalized electrons and/or extended charge resonance, including polymers, charge transfer salts, and mixed valence chains.[71] Instabilities in finite *molecular* systems are also an active research field,[32,40,72,73] where, however, the subtle distinction between static and dynamic effects makes the problem much more complex than in extended systems.[32,55] Here we focus on the spectroscopic consequences of broken-symmetry states in quadrupolar organic dyes for NLO applications. Based on a few-state description of the charge transfer processes that characterize the low-energy physics of these systems and accounting for the coupling between electrons and slow degrees of freedom, including molecular vibrations and effective polar solvation coordinates, we propose a general reference frame to understand the spectroscopic behavior of quadrupolar molecules in solution.

For molecules with a low quadrupolar moment, both the ground and the TPA states are stable. The one-photon allowed state is instead conditionally unstable: for large enough coupling to molecular vibrations, the relevant PES shows two minima corresponding to the two equivalent broken-symmetry structures with polar nature (class **I**). In this case, after vertical excitation the system relaxes towards one of the two minima, leading to a polar relaxed excited state. Polar states are stabilized in polar solvents: symmetry breaking may appear as due to the combined action of vibrational and solvation coupling in systems where vibrational coupling by itself would lead to stable one-photon allowed states. The polar nature of the relaxed OP state is responsible for the positive solvatochromic behavior of steady-state fluorescence observed for this class of dyes, in sharp contrast with the non-solvatochromic absorption spectra.

In dyes with intermediate quadrupolar character (class **II**) the large mixing between neutral and charge separated states guarantees for a sizeable energy splitting between all relevant states, and hence

J. AM. CHEM. SOC. 2006, 128, 15742-15755; DOI: 10.1021/ja064521j

for a good stability of the system. Since all states maintain their non-polar character no major solvatochromic effects are expected for this class of dyes, represented e.g. by squaraine-based dyes. For largely quadrupolar dyes (class **III**) instead the one-photon state is very low in energy and the ground state becomes conditionally unstable. Large inverse solvatochromic behavior is then predicted for these dyes in absorption, whereas fluorescence spectra, occurring from a non-polar state should be unaffected by the solvent polarity.

Many experimental data have been collected for dyes of class **I**: here we discussed a few specific examples. For these dyes we quantitatively account for the large positive solvatochromism observed for steady-state fluorescence spectra and for solvent-independent absorption frequency. More subtle effects, including the lack of mirror-image symmetry between absorption and fluorescence bands, the inhomogeneous broadening of absorption bands in polar solvents, as well as the appearance of vibronically activated TPA features in the region of OP states are naturally understood in the proposed picture. Quantitative agreement with TPA cross-section further validate the picture.

In contrast to chromophores belonging to class **I**, data on chromophores belonging to class **II** are scanty. Our work suggests that squaraine-based dyes belong to this class of molecules. Indeed no major solvatochromism is observed for squaraines neither in absorption nor in fluorescence.[70] Large TPA cross sections are expected for dyes with intermediate quadrupolar character, but care has to be taken, since as $\rho \rightarrow 0.5$ we expect TPA absorption occurring just at twice the energy of the OPA: one-color TPA spectra would then be masked by the OPA signal. To the best of our knowledge, no example of chromophores belonging to class **III** is known: we hope that this work will trigger synthetic effort in this direction. Cyanine-based dyes, with typical absorption in the near-infrared region, usually bear a positive charge, so that the present model is not directly applicable. It is however interesting to notice that for some of these dyes evidences of symmetry breaking in the ground state have been reported in polar solvents.[74]

Solvent-induced symmetry breaking has been recently proposed for the ground state of I_3^-.[72] Whereas

J. AM. CHEM. SOC. 2006, 128, 15742-15755; DOI: 10.1021/ja064521j

this phenomenon is superficially equivalent to our result for chromophores of class **III**, we underline that for I_3^- specific solute-solvent interactions (like, e.g., H-bonds) are considered to be responsible for the phenomenon, while we predict ground- (or excited-) state symmetry breaking in a continuum model for solvation where any site-specific interaction is ruled out. Symmetry breaking in the ground state has been extensively discussed as a consequence of electron-phonon coupling in mixed-valence binuclear metallic complexes.[31,32,55] Indeed relevant models have some common features with our model, the main difference being related to the different nature of the electronic Hamiltonian.

Symmetry breaking (localization) in the excited state is an actively investigated topic in recent years.[18,38,43,44,47,49,75] Specifically, the excited-state symmetry breaking predicted by our model for chromophores of class **I** is in line with recent results reported in Ref. [18], where TD-DFT calculations predict the appearance of broken-symmetry solutions for the relaxed excited state of quadrupolar and octupolar chromophores. Our work generalizes these results for quadrupolar dyes, to account for solvation effects and their consequences in linear and nonlinear spectra. Very recently, the occurrence of symmetry breaking in the excited state of a family of donor-acceptor-donor π-molecules has been discussed based on a phenomenological model.[36] Our microscopic model is based on an essential-state description of the electronic system that represents the reference model for quadrupolar chromophores,[50,51] and can be easily extended to multipolar chromophores. The role of vibrations and solvation coordinates is discriminated, a particularly important issue in view of their different time scales and of their different role in distinguishing between true and false symmetry breaking. In this context, the use of non-adiabatic techniques is instrumental.

The essential-state model adopted here to describe the basic physics of quadrupolar chromophores leads to a *general* phase-diagram for this class of molecules, describing symmetry-breaking phenomena in either the OP excited state or the ground state, as well as cases where symmetry breaking is not supported, neither by electron-vibration coupling nor by solvation interactions. The phase-diagram in Figure 1 can in fact be used to guide the design of chromophores with specific photophysical behavior.

J. AM. CHEM. SOC. 2006, 128, 15742-15755; DOI: 10.1021/ja064521j

For example, if a solvatochromic fluorescence is sought (e.g. for sensing of micropolarity), quite neutral chromophores with sizable electron-phonon coupling should be synthesized; on the contrary, if solvatochromism is not desirable (e.g. when insensitiveness to environment is sought) more quadrupolar chromophores should be designed, quite independently of their electron-phonon coupling. At the same time, based on their solvatochromic behavior, quadrupolar dyes can be easily assigned to one of the three classes in the phase-diagram in Figure 1, so that important information can be obtained on their quadrupolar character (ρ). The value of ρ allows estimating the TPA cross-section, as known by the three-state electronic model.[50] Therefore, the proposed model, via easily accessible experimental data (one-photon absorption and fluorescence), can give important clues on the TPA efficiency of quadrupolar dyes, thus helping the design and the first selection of quadrupolar molecules with optimized properties. For example, chromophores showing no absorption solvatochromism and strong fluorescence solvatochromism already appreciable in slightly polar solvents belong to class **I**, and are expected to have comparatively small TPA cross sections. Quadrupolar chromophores showing appreciable fluorescence solvatochromism only in highly polar solvents can instead be located in region **II** of the phase diagram, but close to region **I** (see example in Figure 2): these dyes have higher TPA cross sections with respect to dyes in region **I**. The best TPA cross sections are expected for chromophores being non-solvatochromic at all, i.e. well within region **II** (intermediate quadrupolar character, like e.g. squaraine dyes). However, in this last case, care has to be taken since as $\rho \square 0.5$ the very intense TP absorption overlaps with the OPA signal, thus suppressing many of the specific features of TPA (such as 3D resolution and linear transparency).

The symmetry breaking phenomenon occurring in the *c*-state as a result of electron-vibration coupling and/or polar solvation is clearly associated with the localization of the excitation in one of the two arms of the chromophore. The problem of localization/delocalization of excitations is a major issue in the study of branched structures, starting from quadrupolar or octupolar chromophores up to all-conjugated dendrimers.[43,45] Understanding the energy transfer processes in such molecules is extremely important

J. AM. CHEM. SOC. 2006, 128, 15742-15755; DOI: 10.1021/ja064521j

with respect to many potential applications. Besides NLO applications, multipolar systems are currently studied as model systems for the mechanism of energy redistribution and the dynamics of electronic coupling in dendritic structures,[43] two basic concepts for controlling the energy flux in order to design and obtain artificial light/energy harvesting systems.[43,76]

The work we presented touches upon several fundamental issues, ranging from vibrationally and/or solvent induced symmetry breaking, to excitation localization/delocalization phenomena, to solvent and vibronic effects in linear and non-linear optical spectra. The proposed model sets the basis to understand the physics of a class of molecules of interest for advanced applications and can be quite easily extended to more complex structures (e.g. octupoles and dendrons): this shall offer a basis to develop reliable guidelines for the synthesis of chromophores and chromophore-based nanoscale systems with optimized properties.

Experimental Section

Synthesis: The synthesis of the bis-donor quadrupole **1** is based on a one-pot double Pd(II)-catalyzed cross-coupling reaction of the fluorene-cored building block 2,7-diethynyl-9,9-dinonyl-9*H*-fluorene with the iodide derivative *N*,*N*-dihexyl-4-iodobenzenamine as described in Ref. [77]. The squarine dye **3** was synthesized from squaric acid and corresponding methylene base, using similar experimental conditions as reported in Ref. [35].

Photophysical Methods: UV/VIS spectra were recorded on a Jasco V-570 spectrophotometer. Fluorescence spectra were obtained at room temperature in dilute solutions (~ 10^{-6} M, taking care that the optical density was less than 0.1, to minimise internal absorption) using an Edinburgh Instruments (FLS 920) spectrometer in photon-counting mode. Emission spectra of compound **1** have been obtained by exciting at the maximum absorption wavelength in each solvent. Excitation wavelength was set to

J. AM. CHEM. SOC. 2006, 128, 15742-15755; DOI: 10.1021/ja064521j

600 nm for compound **3**. Fluorescein in 0.1 N NaOH was used as a standard (quantum yield $\Phi = 0.90$)[78] for determining fluorescence quantum yields.

Two-photon absorption cross-sections (σ_2) were determined by the two-photon-excited fluorescence (TPEF) technique in solution (concentration between 10^{-5} and 10^{-4} M). These measurements provide the TPEF action cross-section $\sigma_2\Phi$. The corresponding σ_2 values were derived by determining the fluorescence quantum yield Φ from standard fluorescence measurements. TPEF measurements were conducted using a mode-locked Ti:sapphire laser operating between 700 and 1000 nm and delivering 120-fs pulses at 76 MHz, following the experimental protocol described in detail by Xu and Webb.[79] Emission was detected in epifluorescence mode, avoiding inner filter effects related to the high dye concentrations by focusing the laser near the cuvette window. Quadratic dependence of the fluorescence intensity on the excitation intensity was verified for each data point. TPEF measurements were calibrated relative to the absolute TPEF action cross-section determined by Xu and Webb for fluorescein in water (pH = 11) in the 690-1000 nm range.[79] Equations for relative determination of σ_2 were adopted as reported in Ref. [80]. Experimental uncertainty does not exceed ± 10%.

Calculation Details. The Hamiltonian in (8) can be numerically diagonalized on the basis obtained by the direct product of the three electronic basis states, $|N\rangle$, $|Z_1\rangle$ and $|Z_2\rangle$, and of the reference vibrational states i.e. the eigenstates of the harmonic oscillators in the last two terms of eq (8). The basis is truncated by fixing a maximum number of phonon states, M; the corresponding $3M\times3M$ matrix can be diagonalized up to fairly large M values, yielding numerically exact nonadiabatic eigenstates. The minimum M required to get convergence depends on the model parameters and on the properties of interest. All results presented in this work have been obtained with $M = 10$.

Linear absorption and fluorescence spectra are calculated by assigning each transition a Gaussian line-shape with half-width at half maximum HWHM. In polar solvents, thermal disorder in the solvation coordinate locally affects the solute properties, so that the solution can be described in terms of a Boltzmann distribution of solute molecules with different ρ, each one in equilibrium with the local

J. AM. CHEM. SOC. 2006, 128, 15742-15755; DOI: 10.1021/ja064521j

configuration of the surrounding solvent. Absorption and emission spectra in polar solvents are then obtained by summing up the spectra calculated for molecules with different ρ, weighted by their Boltzmann probability.[20]

The two-photon absorption cross section is calculated according to the following expression (cgs units):[9,81]

$$\sigma_2(\omega) = \frac{4\pi^2\hbar\omega^2}{c^2 n^2} \mathrm{Im}\langle\gamma(-\omega;\omega,\omega,-\omega)\rangle \qquad (10)$$

where c is the speed of light and n the solvent refractive index and $\langle\gamma\rangle$ the orientationally averaged second hyperpolarizability. This expression is consistent with an expansion of the polarization in a Taylor series with respect to the total electric field:[82]

$$p = p_0 + \alpha \mathrm{E} + \frac{1}{2!}\beta \mathrm{EE} + \frac{1}{3!}\gamma \mathrm{EEE} + \ldots \qquad (11)$$

Tensor elements of $\gamma(-\omega;\omega,\omega,-\omega)$ are given by the following sum-over-states expression:[83]

$$\begin{aligned}\gamma_{ijkl}(-\omega;\omega,\omega,-\omega) = \frac{1}{\hbar^3}\sum_{lmn}\Bigg\{&\frac{\langle g|\mu_i|l\rangle\langle l|\bar{\mu}_j|m\rangle\langle m|\bar{\mu}_k|n\rangle\langle n|\mu_l|g\rangle}{(\Omega_{lg}-\omega)(\Omega_{mg}-2\omega)(\Omega_{ng}-\omega)} + \\ &\frac{\langle g|\mu_j|l\rangle\langle l|\bar{\mu}_i|m\rangle\langle m|\bar{\mu}_k|n\rangle\langle n|\mu_l|g\rangle}{(\Omega^*_{lg}-\omega)(\Omega_{mg}-2\omega)(\Omega_{ng}-\omega)} + \\ &\frac{\langle g|\mu_i|l\rangle\langle l|\bar{\mu}_j|m\rangle\langle m|\bar{\mu}_l|n\rangle\langle n|\mu_k|g\rangle}{(\Omega_{lg}-\omega)(\Omega_{mg}-2\omega)(\Omega_{ng}-\omega)} + \\ &\frac{\langle g|\mu_j|l\rangle\langle l|\bar{\mu}_i|m\rangle\langle m|\bar{\mu}_k|n\rangle\langle n|\mu_l|g\rangle}{(\Omega^*_{lg}-\omega)(\Omega_{mg}-2\omega)(\Omega_{ng}-\omega)}\Bigg\}\end{aligned} \qquad (12)$$

where only two-photon resonant terms have been retained; g is the ground state and summation runs over all excited states; $\Omega_{lg} = \omega_{lg} - i\Gamma_{lg}$ and $\bar{\mu} = \mu - \langle g|\mu|g\rangle$. In our case, the only term different from zero is the γ_{zzzz} term, where z is the axis in the D-A-D direction. The orientationally averaged second hyperpolarizability is thus give by $\langle\gamma\rangle = \frac{1}{5}\gamma_{zzzz}$.[82] Consistently with the Taylor expansion series for the polarizability, expression in (12) is 6 times bigger than the expression one would obtain when

J. AM. CHEM. SOC. 2006, 128, 15742-15755; DOI: 10.1021/ja064521j

expanding the polarization in a perturbative series.[84]

ACKNOWLEDGMENT. Work in Italy was supported by MIUR through FIRB2001 and PRIN2004. We also acknowledge financial support from Rennes Métropole and Délégation Générale pour l'Armement (DGA Grant 00.34.070.00.470.75.653).

Supporting Information Available: Complete reference 7a. This material is available free of charge via the Internet at http://pubs.acs.org.

References

(1) Kanis, D. R.; Ratner, M. A.; Marks, T. J. *Chem. Rev.* **1994,** *94*, 195. Marcus, R. A. *Rev. Mod. Phys.* **1993,** *65*, 599. Myers Kelley, A. *J. Phys. Chem. A* **1999,** *103*, 6891. Brédas, J.-L.; Cornil, K.; Meyers, F.; Beljonne, D. In *Handbook of Conducting Polymers*, Skotheim, T. A.; Elsenbaumer, R. L.; Reynolds, J. R., Ed.; Marcel Dekker: New York, 1998; Vol. 1, p 1.

(2) Reichardt, C. *Chem. Rev.* **1994,** *94*, 2319.

(3) Del Zoppo, M.; Castiglioni, C.; Zerbi, G. In *Handbook of Conducting Polymers*, Skotheim, T. A.; Elsenbaumer, R. L.; Reynolds, J. R., Ed.; Marcel Dekker: New York, 1998; Vol. 1, p 765.

(4) Marder, S. R.; Beratan, D. N.; Cheng, L. T. *Science* **1991,** *252*, 103. Lin, T.-C.; He, G. S.; Prasad, P. N.; Tan, L.-S. *J. Mater. Chem.* **2004,** *14*, 982. Reinhardt, B. A.; Brott, L. L.; Clarson, S. J.; Dillard, A. G.; Bhatt, J. C.; Kannan, R.; Yuan, L.; He, G. S.; Prasad, P. N. *Chem. Mater.* **1998,** *10*, 1863. Belfield, K. D.; Schafer, K. J.; Mourad, W.; Reinhardt, B. A. *J. Org. Chem.* **2000,** *65*, 4475. Beverina, L.; Fu, J.; Leclercq, A.; Zojer, E.; Pacher, P.; Barlow, S.; Van Stryland, E. W.; Hagan, D. J.; Brédas, J.-L.; Marder, S. R. *J. Am. Chem. Soc.* **2005,** *127*, 7282.

(5) Antonov, L.; Kamada, K.; Ohta, K.; Kamounah, F. S. *Phys. Chem. Chem. Phys.* **2003,** *5*, 1193.

(6) He, G. S.; Xu, G. C.; Prasad, P. N.; Reinhardt, B. A.; Bhatt, J. C.; McKellar, R.; Dillard, A. G. *Opt. Lett.* **1995,** *20*, 435. Kim, O.-K.; Lee, K.-S.; Woo, H. Y.; Kim, K.-S.; He, G. S.; Guang, S. H.; Swiatkiewicz, J.; Prasad, P. N. *Chem. Mater.* **2000,** *12*, 284. Chung, S.-J.; Rumi, M.; Alain, V.; Barlow, S.; Perry, J. W.; Marder, S. R. *J. Am. Chem. Soc.* **2005,** *127*, 10844. Charlot, M.; Izard, N.; Mongin, O.; Riehl, D.; Blanchard-Desce, M. *Chem. Phys. Lett.* **2006,** *417*, 297. Charlot, M.; Porrès, L.; Entwistle, C. D.; Beeby, A.; Marder, T. B.; Blanchard-Desce, M. *Phys. Chem. Chem. Phys.* **2005,** *7*, 600. Frederiksen, P. K.; Jørgensen, M.; Ogilby, P. R. *J. Am. Chem. Soc.* **2001,** *123*, 1215. Abbotto, A.; Beverina, L.; Bozio, R.; Facchetti, A.; Ferrante, C.; Pagani, G. A.; Pedron, D.; Signorini, R. *Org. Lett.* **2002,** *4*, 1495. Kim, O. K.; Lee, K. S.; Huang, Z.; Heuer, W. B.; Paik-Sung, C. S. *Opt. Mater.* **2003,** *21*, 559. Iwase, Y.; Kamada, K.; Ohta, K.; Kondo, K. *J. Mater. Chem.* **2003,** *13*, 1575. Kawamata, J.; Akiba, M.; Tani, T.; Harada, A.; Inagaki, Y. *Chem. Lett.* **2004,** *33*, 448. Strehmel, B.; Amthor, S.; Schelter, J.; Lambert, C. *ChemPhysChem* **2005,** *6*, 893.

(7) Albota, M. et al. *Science* **1998,** *281*, 1653. Werts, M. H. V.; Gmouh, S.; Mongin, O.; Pons, T.; Blanchard-Desce, M. *J. Am. Chem. Soc.* **2004,** *126*, 16294. Pond, S. J. K.; Rumi, M.; Levin, M. D.; Parker, T. C.; Beljonne, D.; Day, M. W.; Brédas, J.-L.; Marder, S. R.; Perry, J. W. *J. Phys. Chem. A* **2002,** *106*, 11470. Yang, W. J.; Kim, D. Y.; Jeong, M.-Y.; Kim, H. M.; Jeon, S.-J.; Cho, B. R. *Chem. Commun.* **2003**, 2618.

(8) Ventelon, L.; Charier, S.; Moreaux, L.; Mertz, J.; Blanchard-Desce, M. *Angew. Chem., Int. Ed.* **2001,** *40*, 2098.

(9) Rumi, M.; Ehrlich, J. E.; Heikal, A. A.; Perry, J. W.; Barlow, S.; Hu, Z.-Y.; McCord-Maughon,

J. AM. CHEM. SOC. 2006, 128, 15742-15755; DOI: 10.1021/ja064521j

D.; Parker, T. C.; Röckel, H.; Thayumanavan, S.; Marder, S. R.; Beljonne, D.; Brédas, J.-L. *J. Am. Chem. Soc.* **2000,** *122*, 9500.
(10) Woo, H. Y.; Liu, B.; Kohler, B.; Korystov, D.; Mikhailovsky, A.; Bazan, G. C. *J. Am. Chem. Soc.* **2005,** *127*, 14721.
(11) Ventelon, L.; Blanchard-Desce, M.; Moreaux, L.; Mertz, J. *Chem. Commun.* **1999**, 2055.
(12) Mongin, O.; Porrès, L.; Moreaux, L.; Mertz, J.; Blanchard-Desce, M. *Org. Lett.* **2002,** *4*, 719.
(13) Strehmel, B.; Sarker, A. M.; Detert, H. *ChemPhysChem* **2003,** *4*, 249.
(14) Zyss, J.; Ledoux, I. *Chem. Rev.* **1994,** *94*, 77. Joshi, M. P.; Swiatkiewicz, J.; Xu, F.; Prasad, P. N.; Reinhardt, B. A.; Kannan, R. *Opt. Lett.* **1998,** *23*, 1742. He, G. S.; Swiatkiewicz, J.; Jiang, Y.; Prasad, P. N.; Reinhardt, B. A.; Tan, L.-S.; Kannan, R. *J. Phys. Chem. A* **2000,** *104*, 4805. Yang, W. J.; Kim, D. Y.; Kim, C. H.; Jeong, M.-Y.; Lee, S. K.; Jeon, S.-J.; Cho, B. R. *Org. Lett.* **2004,** *6*, 1389. Parent, M.; Mongin, O.; Kamada, K.; Katan, K.; Blanchard-Desce, M. *Chem. Commun.* **2005**, 2029.
(15) Chung, S.-J.; Kim, K.-S.; Lin, T.-C.; He, G. S.; Swiatkiewicz, J.; Prasad, P. N. *J. Phys. Chem. B* **1999,** *103*, 10741. Cho, B. R.; Son, K. H.; Sang, H. L.; Song, Y.-S.; Lee, Y.-K.; Jeon, S.-J.; Choi, J. H.; Lee, H.; Cho, M. *J. Am. Chem. Soc.* **2001,** *123*, 10039. Beljonne, D.; Wenseleers, W.; Zojer, E.; Shuai, Z.; Vogel, H.; Pond, S. J. K.; Perry, J. W.; Marder, S. R.; Brédas, J.-L. *Adv. Funct. Mater.* **2002,** *12*, 631. Mongin, O.; Porrès, L.; Katan, C.; Pons, T.; Mertz, J.; Blanchard-Desce, M. *Tetrahedron Lett.* **2003,** *44*, 8121. Porrès, L.; Mongin, O.; Katan, C.; Charlot, M.; Pons, T.; Mertz, J.; Blanchard-Desce, M. *Org. Lett.* **2004,** *6*, 47. Lee, H. J.; Sohn, J.; Hwang, J.; Park, S. Y.; Choi, H.; Cha, M. *Chem. Mater.* **2004,** *16*, 456. Meng, F.; Li, B.; Qian, S.; Chen, K.; Tian, H. *Chem. Lett.* **2004,** *33*, 470.
(16) Mongin, O.; Brunel, J.; Porrès, L.; Blanchard-Desce, M. *Tetrahedron Lett.* **2003,** *44*, 2813.
(17) Le Droumaguet, C.; Mongin, O.; Werts, M. H. V.; Blanchard-Desce, M. *Chem. Commun.* **2005**, 2802.
(18) Katan, C.; Terenziani, F.; Mongin, O.; Werts, M. H. V.; Porrès, L.; Pons, T.; Mertz, J.; Tretiak, S.; Blanchard-Desce, M. *J. Phys. Chem. A* **2005,** *109*, 3024.
(19) Liptay, W. *Angew. Chem. Int. Ed.* **1969,** *8*, 177.
(20) Boldrini, B.; Cavalli, E.; Painelli, A.; Terenziani, F. *J. Phys. Chem. A* **2002,** *106*, 6286.
(21) Painelli, A.; Terenziani, F. *Chem. Phys. Lett.* **1999,** *312*, 211.
(22) Painelli, A.; Terenziani, F. *J. Phys. Chem. A* **2000,** *104*, 11041.
(23) Terenziani, F.; Painelli, A.; Comoretto, D. *J. Phys. Chem. A* **2000,** *104*, 11049.
(24) Bishop, D. M. *Adv. Chem. Phys.* **1998,** *104*, 1. Macak, P.; Luo, Y.; Norman, P.; Ågren, H. *J. Chem. Phys.* **2000,** *113*, 7055. Macak, P.; Luo, Y.; Ågren, H. *Chem. Phys. Lett.* **2000,** *330*, 447. Kim, H.-S.; Cho, M.; Jeon, S.-J. *J. Chem. Phys.* **1997,** *107*, 1936. Painelli, A.; Del Freo, L.; Terenziani, F. In *Nonlinear Optical Responses of Molecules, Solids and Liquids: Methods and Applications*, Papadopoulos, M., Ed.; Research Signpost: India, 2003; Vol. 1, p 39.
(25) Painelli, A. *Chem. Phys. Lett.* **1998,** *285*, 352.
(26) Del Freo, L.; Terenziani, F.; Painelli, A. *J. Chem. Phys.* **2002,** *116*, 755.
(27) Mulliken, R. S. *J. Am. Chem. Soc.* **1952,** *74*, 811. Mulliken, R. S.; Person, W. B., *Molecular Complexes: A Lecture and Reprint Volume*. Wiley: New York, 1969; Vol. 1.
(28) Soos, Z. G.; Klein, D. J. In *Molecular Association: Including Molecular Complexes*, Foster, R., Ed.; Academic Press: New York, 1975; Vol. 1, p 1. Soos, Z. G.; Bewick, S. A.; Peri, A.; Painelli, A. *J. Chem. Phys.* **2004,** *120*, 6712.
(29) Clark, R. J. H. In *Advances in Infrared and Raman Spectroscopy*, Clark, R. J. H.; Hester, R. E., Ed.; Wiley: New York, 1984; Vol. 2, p 95. Hush, N. S. *Prog. Inorg. Chem.* **1967,** *8*, 391. Creutz, C. *Prog. Inorg. Chem.* **1983,** *30*, 1.
(30) Gammel, J. T.; Saxena, A.; Batistic, I.; Bishop, A. R.; Phillpot, S. R. *Phys. Rev. B* **1992,** *45*, 6408. Bozio, R.; Pecile, C. In *Spectroscopy of Advanced Materials, Advances in Spectroscopy*, Clark, R. J. H.; Hester, R. E., Ed.; Wiley: New York, 1991; Vol. 19, p 1. Painelli, A.; Girlando, A. *Phys. Rev. B* **1992,** *45*, 8913. Anusooya-Pati, Y.; Soos, Z. G.; Painelli, A. *Phys. Rev. B* **2001,**

J. AM. CHEM. SOC. 2006, 128, 15742-15755; DOI: 10.1021/ja064521j

63, 205118. Egami, T.; Ishihara, S.; Tachiki, M. *Science* **1993,** *261*, 1307. Egami, T.; Tachiki, M. *Phys. Rev. B* **1994,** *49*, 8944.
(31) Prassides, K.; Schatz, P. N.; Wong, K. Y.; Day, P. *J. Phys. Chem. B* **1986,** *90*, 5588.
(32) Ferretti, A.; Lami, A.; Ondrechen, M. J.; Villani, G. *J. Chem. Phys.* **1995,** *99*, 10484.
(33) Belfield, K. D.; Hagan, D. J.; Van Stryland, E. W.; Schafer, K. J.; Negres, R. A. *Org. Lett.* **1999,** *1*, 1575. Zojer, E.; Wenseleers, W.; Pacher, P.; Barlow, S.; Halik, M.; Grasso, C.; Perry, J. W.; Marder, S. R.; Brédas, J.-L. *J. Phys. Chem. B* **2004,** *108*, 8641.
(34) Verbouwe, W.; Viaene, L.; Van der Auweraer, M.; De Schryver, F. C.; Masuhara, H.; Pansu, R.; Faure, J. *J. Phys. Chem. A* **1997,** *101*, 8157.
(35) Scherer, D.; Dörfler, R.; Feldner, A.; Vogtmann, T.; Schwoerer, M.; Lawrentz, U.; Grahn, W.; Lambert, C. *Chem. Phys.* **2002,** *279*, 179.
(36) Amthor, S.; Lambert, C.; Dümmler, S.; Fischer, I.; Schelter, J. *J. Phys. Chem. A* **2006,** *110*, 5204.
(37) Abbotto, A.; Beverina, L.; Bozio, R.; Facchetti, A.; Ferrante, C.; Pagani, G. A.; Pedron, D.; Signorini, R. *Chem. Commun.* **2003**, 2144. Brunel, J.; Mongin, O.; Jutand, A.; Ledoux, I.; Zyss, J.; Blanchard-Desce, M. *Chem. Mater.* **2003,** *15*, 4139. Cho, B. R.; Lee, S. J.; Lee, S. H.; Son, K. H.; Kim, Y. H.; Doo, J.-Y.; Lee, G. J.; Kang, T. I.; Lee, Y. K.; Cho, M.; Jeon, S.-J. *Chem. Mater.* **2001,** *13*, 1438. Chung, S.-J.; Lin, T.-C.; Kim, K.-S.; He, G. S.; Swiatkiewicz, J.; Prasad, P. N.; Baker, G. A.; Bright, F. V. *Chem. Mater.* **2001,** *13*, 4071. Lambert, C.; Gaschler, W.; Schmälzlin, E.; Meerholz, K.; Bräuchle, C. *J. Chem. Soc., Perkin Trans. 2* **1999,** *2*, 577. Lee, W.-H.; Lee, H.; Kim, J.-A.; Choi, J.-H.; Cho, M.; Jeon, S.-J.; Cho, B. R. *J. Am. Chem. Soc.* **2001,** *123*, 10658. Stadler, S.; Feiner, F.; Bräuchle, C.; Brandl, S.; Gompper, R. *Chem. Phys. Lett.* **1995,** *245*, 292.
(38) Lahankar, S. A.; West, R.; Varnavski, O.; Xie, X.; Goodson III, T. *J. Chem. Phys.* **2004,** *120*, 337.
(39) Verbouwe, W.; Van der Auweraer, M.; De Schryver, F. C.; Piet, J. J.; Warman, J. M. *J. Am. Chem. Soc.* **1998,** *120*, 1319.
(40) Liu, L. A.; Peteanu, L. A.; Yaron, D. J. *J. Phys. Chem. B* **2004,** *108*, 16841.
(41) Bangal, P. R.; Lam, D. M. K.; Peteanu, L. A.; Van der Auweraer, M. *J. Phys. Chem. B* **2004,** *108*, 16834.
(42) Verbeek, G.; Depaemelaere, S.; Van der Auweraer, M.; De Schryver, F. C.; Vaes, A.; Terrell, D.; De Meutter, S. *Chem. Phys.* **1993,** *176*, 195.
(43) Goodson III, T. G. *Acc. Chem. Res.* **2005,** *38*, 99.
(44) Varnavski, O. P.; Ostrowski, J. C.; Sukhomlinova, L.; Twieg, R. J.; Bazan, G., C.; Goodson III, T. *J. Am. Chem. Soc.* **2002,** *124*, 1736.
(45) Wang, Y.; He, G. S.; Prasad, P. N.; Goodson III, T. *J. Am. Chem. Soc.* **2005,** *127*, 10128.
(46) Adronov, A.; Fréchet, J. M. J.; He, G. S.; Kim, K.-S.; Chung, S.-J.; Swiatkiewicz, J.; Prasad, P. N. *Chem. Mater.* **2000,** *12*, 2838. Brousmiche, D. W.; Serin, J. M.; Fréchet, J. M. J.; He, G. S.; Lin, T.-C.; Chung, S.-J.; Prasad, P. N.; Kannan, R.; Tan, L.-S. *J. Phys. Chem. B* **2004,** *108*, 8592. Díez-Barra, E.; García-Martínez, J. C.; Merino, S.; del Rey, R.; Rodríguez-López, J.; Sánchez-Verdú, P.; Tejeda, J. *J. Org. Chem.* **2001,** *66*, 5664. Drobizhev, M.; Karotki, A.; Rebane, A.; Spangler, C. W. *Opt. Lett.* **2001,** *26*, 1081. Drobizhev, M.; Karotki, A.; Dzenis, Y.; Rebane, A.; Suo, Z.; Spangler, C. W. *J. Phys. Chem. B* **2003,** *107*, 7540. Ma, H.; Jen, A. K.-Y. *Adv. Mater.* **2001,** *13*, 1201. Meier, H.; Lehmann, M.; Kolb, U. *Chem. Eur. J.* **2000,** *6*, 2462. Ranasinghe, M. I.; Varnavski, O. P.; Pawlas, J.; Hauck, S. I.; Louie, J.; Hartwig, J. F.; Goodson, T., III *J. Am. Chem. Soc.* **2002,** *124*, 6520. Segura, J. L.; Gómez, R.; Martín, N.; Guldi, D. M. *Org. Lett.* **2001,** *3*, 2645. Spangler, C. W.; Suo, Z.; Drobizhev, M.; Karotki, A.; Rebane, A. *NATO Science Series, II: Mathematics, Physics and Chemistry* **2003,** *100*, 139. Wang, Y.; Ranasinghe, M. I.; Goodson, T., III *J. Am. Chem. Soc.* **2003,** *125*, 9562. Mongin, O.; Rama Krishna, T.; Werts, M. H. V.; Caminade, A.-M.; Majoral, J.-P.; Blanchard-Desce, M. *Chem. Commun.* **2006**, 915.

J. AM. CHEM. SOC. 2006, 128, 15742-15755; DOI: 10.1021/ja064521j

(47) Gaab, K. M.; Thompson, A. L.; Xu, J.; Martínez, T. J.; Bardeen, C. J. *J. Am. Chem. Soc.* **2003,** *125*, 9288. Thompson, A. L.; Gaab, K. M.; Xu, J.; Bardeen, C. J.; Martínez, T. J. *J. Phys. Chem. A* **2004,** *108*, 671.
(48) Detert, H.; Sugiono, E.; Kruse, G. *J. Phys. Org. Chem.* **2002,** *15*, 638. Detert, H.; Schmitt, V. *J. Phys. Org. Chem.* **2004,** *17*, 1051.
(49) Stahl, R.; Lambert, C.; Kaiser, C.; Wortmann, R.; Jakober, R. *Chem. Eur. J.* **2006,** *12*, 2358.
(50) Barzoukas, M.; Blanchard-Desce, M. *J. Chem. Phys.* **2000,** *113*, 3951.
(51) Hahn, S.; Kim, D.; Cho, M. *J. Phys. Chem. B* **1999,** *103*, 8221.
(52) Thompson, W. H.; Blanchard-Desce, M.; Alain, V.; Muller, J.; Fort, A.; Barzoukas, M.; Hynes, J. T. *J. Phys. Chem. A* **1999,** *103*, 3766. Thompson, W. H.; Blanchard-Desce, M.; Hynes, J. T. *J. Phys. Chem. A* **1998,** *102*, 7712. Barzoukas, M.; Runser, C.; Fort, A.; Blanchard-Desce, M. *Chem. Phys. Lett.* **1996,** *257*, 531.
(53) Leng, W.; Würthner, F.; Myers Kelley, A. *J. Phys. Chem. A* **2005,** *109*, 1570. Moran, A. M.; Egolf, D. S.; Blanchard-Desce, M.; Myers Kelley, A. *J. Chem. Phys.* **2002,** *116*, 2542. Biswas, N.; Umapathy, S. *Chem. Phys. Lett.* **1998,** *294*, 181. Lu, D.; Che, G.; Perry, J. W.; Goddard III, W. A. *J. Am. Chem. Soc.* **1994,** *116*, 10679. Kim, H.-S.; Cho, M.; Jeon, S.-J. *J. Chem. Phys.* **1997,** *107*, 1936. Cho, M. *J. Phys. Chem. A* **1999,** *103*, 4712. Terenziani, F.; Painelli, A.; Girlando, A.; Metzger, R. M. *J. Phys. Chem. B* **2004,** *108*, 10743.
(54) Moran, A. M.; Delbecque, C.; Myers Kelley, A. *J. Phys. Chem. A* **2001,** *105*, 10208. Terenziani, F.; Mongin, O.; Katan, C.; Bhatthula, B. K. G.; Blanchard-Desce, M. *Chem. Eur. J.* **2006,** *12*, 3089. Terenziani, F.; Morone, M.; Gmouh, S.; Blanchard-Desce, M. *ChemPhysChem* **2006,** *7*, 685.
(55) Zhang, Q.; Silbey, R. *J. Chem. Phys.* **1990,** *92*, 4899.
(56) Borghi, G. P.; Girlando, A.; Painelli, A.; Voit, J. *Europhys. Lett.* **1996,** *34*, 127.
(57) Onsager, L. *J. Am. Chem. Soc.* **1936,** *58*, 1486.
(58) Painelli, A. *Chem. Phys.* **1999,** *245*, 185.
(59) Moran, A. M.; Myers Kelley, A. *J. Chem. Phys.* **2001,** *115*, 912.
(60) Mukamel, S., *Principles of Nonlinear Optical Spectroscopy*. Oxford University Press: 1999; Vol. 1.
(61) Mongin, O.; Charlot, M.; Katan, C.; Porrès, L.; Parent, M.; Pons, T.; Mertz, J.; Blanchard-Desce, M. *Proc. SPIE-Int. Soc. Opt. Eng.* **2004,** *5516*, 9.
(62) Ventelon, L.; Moreaux, L.; Mertz, J.; Blanchard-Desce, M. *Synth. Met.* **2002,** *127*, 17. Porrès, L.; Mongin, O.; Katan, C.; Charlot, M.; Bhatthula, B. K. G.; Jouikov, V.; Pons, T.; Mertz, J.; Blanchard-Desce, M. *J. Nonlinear Opt. Phys.* **2004,** *13*, 451. Silly, M. G.; Porrès, L.; Mongin, O.; Chollet, P.-A.; Blanchard-Desce, M. *Chem. Phys. Lett.* **2003,** *379*, 74. Porrès, L.; Katan, C.; Mongin, O.; Pons, T.; Mertz, J. *J. Mol. Struct.* **2004,** *704*, 17.
(63) Katan, C.; Tretiak, S.; Bain, A.; Werts, M.; Mongin, O.; Blanchard-Desce, M.; unpublished results.
(64) Reynolds, L.; Gardecki, J. A.; Frankland, S. J. V.; Horng, M. L.; Maroncelli, M. *J. Phys. Chem.* **1996,** *100*, 10337.
(65) Sluch, M. I.; Godt, A.; Bunz, U. H. F.; Berg, M. A. *J. Am. Chem. Soc.* **2001,** *123*, 6447.
(66) Lippert, E. *Z. Naturforsch. A* **1955,** *10*, 541. Mataga, N.; Kaifu, Y.; Koizumi, M. *Bull. Chem. Soc. Jpn.* **1955,** *28*, 690.
(67) Strickler, S. J.; Berg, R. A. *J. Chem. Phys.* **1962,** *37*, 814.
(68) The calculated position for the TPA band is probably slightly red-shifted with respect to what can be experimentally estimated, but this goes with the parallel shift of the OPA band (see the previously discussed Stokes-shift problem).
(69) Suppan, P. *J. Photochem. Photobiol., A* **1990,** *50*, 293. Ghoneim, N.; Suppan, P. *Spectrochim. Acta, Part A* **1995,** *51A*, 1043. Suppan, P.; Ghoneim, N., *Solvatochromism*. Royal Society of Chemistry: Cambridge, England, 1997; Vol. 1.
(70) Zhao, W.; Hou, Y. J.; Wang, X. S.; Zhang, B. W.; Cao, Y.; Yang, R.; Wang, W. B.; Xiao, X. R.

J. AM. CHEM. SOC. 2006, 128, 15742-15755; DOI: 10.1021/ja064521j

Sol. Energy Mater. Sol. Cells **1999,** *58*, 173. Dirk, C. W.; Herndon, W. C.; Cervantes-Lee, F.; Selnau, H.; Martinez, S.; Kalamegham, P.; Tan, A.; Campos, G.; Velez, M.; Zyss, J.; Ledoux, I.; Chengg, L.-T. *J. Am. Chem. Soc.* **1995,** *117*, 2214. Das, S.; Thomas, K. G.; Ramanathan, R.; George, M. V.; Kamat, P. V. *J. Phys. Chem.* **1993,** *97*, 13625. Gude, C.; Rettig, W. *J. Phys. Chem. A* **2000,** *104*, 8050. Cornelissen-Gude, C.; Rettig, W.; Lapouyade, R. *J. Phys. Chem. A* **1997,** *101*, 9373. Tatikolov, A. S.; Costa, S. M. B. *J. Photochem. Photobiol., A* **2001,** *140*, 147–156.

(71) Painelli, A.; Girlando, A. *J. Chem. Phys.* **1986,** *84*, 5665. Girlando, A.; Painelli, A.; Soos, Z. G. *Acta Phys. Pol., A* **1995,** *87*, 735. Soos, Z. G.; Mukhopadhyay, D.; Painelli, A.; Girlando, A. In *Handbook of Conducting Polymers*, Skotheim, T. A.; Elsenbaumer, R. L.; Reynolds, J. R., Ed.; Marcel Dekker: New York, 1998; Vol. 1, p 165.

(72) Zhang, F. S.; Lynden-Bell, R. M. *Phys. Rev. Lett.* **2003,** *90*, 185505.

(73) Myers Kelley, A.; Shoute, L. C. T.; Blanchard-Desce, M.; Bartholomew, G. P.; Bazan, G. *Mol. Phys.* **2006,** *104*, 1239.

(74) Tolbert, L. M.; Zhao, X. *J. Am. Chem. Soc.* **1997,** *119*, 3253. Furuya, K.; Inagaki, Y.; Torii, H.; Furukawa, Y.; Tasumi, M. *J. Phys. Chem. A* **1998,** *102*, 8413. Lepkowicz, R. S.; Przhonska, O. V.; Hales, J. M.; Fu, J.; Hagan, D. J.; Stryland, E. W. V.; Bondar, M. V.; Slominsky, Y. L.; Kachkovski, A. D. *Chem. Phys.* **2004,** *305*, 259–270.

(75) Franco, I.; Tretiak, S. *J. Am. Chem. Soc.* **2004,** *126*, 12130. Tretiak, S.; Saxena, A.; Martin, R. L.; Bishop, A. R. *Phys. Rev. Lett.* **2002,** *89*, 097402.

(76) Bar-Haim, A.; Klafter, J.; Kopelman, R. *J. Am. Chem. Soc.* **1997,** *119*, 6197.

(77) Mongin, O.; Porrès, L.; Charlot, M.; Katan, C.; Blanchard-Desce, M. *Chem. Eur. J.*, in press.

(78) Demas, J. N.; Crosby, G. A. *J. Phys. Chem.* **1971,** *75*, 991.

(79) Xu, C.; Webb, W. W. *J. Opt. Soc. Am. B* **1996,** *13*, 481.

(80) Werts, M. H. V.; Nerambourg, N.; Pélégry, D.; Grand, Y. L.; Blanchard-Desce, M. *Photochem. Photobiol. Sci.* **2005,** *4*, 531.

(81) Sutherland, R. L., *Handbook of Nonlinear Optics*. Marcel Dekker: New York, 1996; Vol. 1.

(82) Brédas, J.-L.; Adant, C.; Tackx, P.; Persoons, A. *Chem. Rev.* **1994,** *94*, 243. Cyvin, S. J.; Rauch, J. E.; Decius, J. C. *J. Chem. Phys.* **1965,** *43*, 4083.

(83) Orr, B. J.; Ward, J. F. *Mol. Phys.* **1971,** *20*, 513.

(84) Butcher, P. N.; Cotter, D., *The Elements of Nonlinear Optics*. Cambridge University Press: Cambridge, 1990; Vol. 1. Willetts, A.; Rice, J. E.; Burland, D. M.; Shelton, D. P. *J. Chem. Phys.* **1992,** *97*, 7590.

J. AM. CHEM. SOC. 2006, 128, 15742-15755; DOI: 10.1021/ja064521j

Table of content graphic

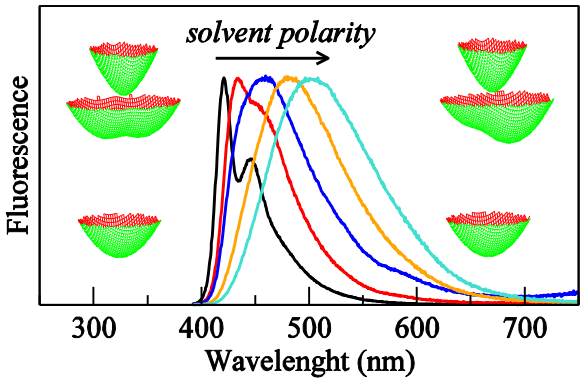

J. AM. CHEM. SOC. 2006, 128, 15742-15755; DOI: 10.1021/ja064521j